ACCRETION DISKS IN THE CATALYSMIC VARIABLES

by

M.C. Koen

Submitted in fulfilment of the requirements
for the M.Sc. degree at the
University of Cape Town

June, 1976

Acknowledgements

I am grateful to Professor B. Warner, both for suggesting the topic and for many helpful suggestions; to John Brickhill for providing a program subroutine and to Patrick Hurly and Neels Erasmus for advice on computing.

The financial assistance of the C.S.I.R. is acknowledged.

SUMMARY

The general equations describing the time-independent structure of gaseous circumstellar disks in vertical hydrostatic equilibrium are derived. The possibility of turbulent instablilty and the resulting viscosity laws are discussed.

The set of coupled partial differential equations is simplified to two simultaneous ordinary differential equations for temperature and density. Computer solutions are given for parameters consistent with a white dwarf central star ($1M_\odot$, radius 10^9 cm) for accretion rates 10^{17} and 10^{18} g sec^{-1}. The viscosity law of Shakura & Sunyaev (1973) was used and energy transfer by radiation, convection and turbulence was included. Although the assumed constancy of the mean molecular weight and the adiabaticity of convection are doubtful, other assumptions are satisfied within large margins.

Disks are found to be optically thick and geometrically thin (half thickness $\lesssim 4 \times 10^9$ cm). The discrepancy between the disk masses derived here ($M_d \sim 10^{22} - 10^{24}$ g) and those found by other authors is discussed. Model results are used to calculate the profile of the H_β absorption line produced in the disk. This is done by a numerical integration over the disk volume for a range of inclination angles and disk radii. Thermal and rotational Doppler broadening as well as pressure broadening are taken into account. Accurate monochromatic absorption coefficients are used.

Computed line profiles show fair qualitative agreement with those observed in LS 55^o-8 and TT Ari, lending support to the suggestion of Warner (1975) that absorption lines in

the cataclysmic variables originate in the disk. Reasonable agreement between theoretical and observed continuum spectra is found for Z Cam and AR And, but the model disks are unable to produce the soft X-ray flux observed in SS Cyg.

It is concluded that the order of magnitude of the viscosity can, at present, not be established by comparison of theory and observations unless models are extended to

(i) systems other than cataclysmic variables, or

(ii) the calculation of emission spectra or absorption lines of heavy elements.

OPSOMMING

Die vergelykings wat die tyd-onafhanklike struktuur van gasskywe om sterre beskryf word afgelei. Daar word aangeneem dat die skywe in hidrostatiese ewewig in die vertikale rigting verkeer. Die moontlikheid van turbulente onstabiliteit en voortspruitende viskositeitswette word bespreek.

Die stel onderling-afhanklike parsiële differensiaal-vergelykings word vereenvoudig na twee gelyktydige gewone differensiaalvergelykings met temperatuur en digtheid as afhanklike veranderlikes. Rekenaaroplossings vir kenmerkende wit-dwerg-parameters ($1M_{\odot}$, straal 10^9 cm) word gegee vir massavloei-tempos 10^{17} en 10^{18} g s^{-1}. Die viskositeitsverband van Shakura & Sunyaev (1973) is gebruik en energie-oordrag deur straling, stroming en turbulente bewegings is in ag geneem. Met die moontlike uitsondering van die aannames dat die gemiddelde molekulêre gewig konstant is en dat stroming adiabaties is, staaf resultate die benaderings wat gemaak is.

Die resultate toon dat skywe groot ondeursigtigheid en klein halfdiktes ($\lesssim 4 \times 10^9$ cm) het. Moontlike oorsake van die verskil tussen skyfmassas hier bereken ($M_d \sim 10^{22} - 10^{24}$ g) en waardes afgelei deur ander werkers word bespreek.

Resultate van die modelkonstruksies word gebruik om die profiele van die H_β-absorpsielyn wat in the skyf gevorm word te bereken. Dit word vermag deur 'n integraal oor die volume van die skyf numeries te bepaal. Die proses is uitgevoer vir 'n reeks hellings en radiale groottes van die skyf. Lynverbreding deur termiese-en rotasie-Dopplerverskuiwings asook drukverbreding is in ag geneem. Akkurate monochromatiese

absorpsiekoëffisiënte is gebruik.

Die feit dat berekende profiele kwalitatief ooreenstem met dié waargeneem in LS 55° -8 en TT Ari kan as steun vir Warner (1975) se voorstel (dat absorpsielyne in die kataklismiese veranderlikes in 'n gasskyf ontstaan) gesien word. Redelike ooreenstemming tussen teoretiese en waargenome deurlopende spektra word verkry vir die sisteme Z Cam en AR And, hoewel berekeninge nie die waargenome lang-X-straalvloed (soos waargeneem in SS Cyg) voorspel nie.

Die slotsom is dat tensy toepassing van die teorie hier bespreek op óf ander soorte gasskywe óf die berekeninge van ander lynprofiele nuwe feite aan die dag bring, dit op die huidige stadium nie moontlik is om die orde-grootte van die viskositeitskoëffisiënt aan die hand van waarnemings te bepaal nie.

Contents

I. Introduction

Description of the contemporary model for cataclysmic variables (CVs)

We will define cataclysmic variables to be classical, recurrent and dwarf novae and novalike variables. Although exhibiting a wide range of outburst amplitudes and recurrence periods (e.g. Payne-Gaposchkin (1964)), a common model based on spectroscopic and photometric similarities has been evolved. Briefly; all systems are close binaries consisting of a white dwarf (primary) and a main sequence companion of types G to M (secondary). With the exception of T Cr B binary periods are of the order of a few hours (Mumford 1967). The secondary component fills its Roche Lobe and loses hydrogen rich material to the white dwarf through the inner Lagrangian point (Kraft 1963). Since angular momentum has to be conserved the transferred matter eventually forms an optically thick disk around the primary; the region where the gas stream intersects the disk is observable as a bright spot (Warner & Nather 1971, Flannery 1974). The quasi-periodic flickering in light output from the system is attributed to the hot spot, and is probably caused by inhomogeneities in, or modulation of the accretion stream (Gorbatsky 1969). Outbursts are associated with the white dwarf component (Warner 1973).

Motivation for theoretical studies of accretion disks in CVs

We mention a few problems posed by observations the resolution of which will probably require a reliable disk model.

1) Outburst mechanism

In the case of recurrent and classical novae, the outburst model of Starrfield et al. (1972) is well accepted. A thermal runaway followed by explosive nuclear burning on the white dwarf surface. Controversy remains in the dwarf nova case; we shall discuss three prominent models here.

Starrfield et al. (1974a,b) and Warner (1974) have suggested a variant of the nova model in which the disk is heated by a propagating shock wave: the shock is formed when the supersonically expanding envelope of the white dwarf impacts on the disk after nuclear burning. The model is successful in explaining observations such as the Parenago-Kukarkin relation between recurrence period and magnitude of outburst, and the increase in disk size during outburst. The model has been criticized on theoretical grounds by Sparks & Starrfield (1975) and Bath et al. (1974). In particular, the latter claim that shock propagation through a centrifugally supported disk is unlikely.

Bath et al. (1974), Bath (1973) propose that the brightening is due to an increase in the mass flux through the disk. This could be as a result of stimulated mass loss from the red component, induced by quasi-periodic dynamical instabilities (Bath & Papaloizou 1975). Standstills in Z Cam stars and the absence of minor outbursts in novae are then indicative of steady accretion. Osaki (1974) postulates outbursts due to an increased mass flux onto the white dwarf, liberating a large amount of gravitational energy. The large flow of matter is caused by an unknown instability in the disk.

2) Periodicities

Short period pulsations (~17-115 seconds) have been found in several CV-systems. In dwarf novae these periodicities are present only during or directly after outbursts. The origin of the pulsations has been ascribed to non-radial oscillations of the white dwarf (Warner & Robinson 1972), magnetic funnelling causing hot spots on the dwarf surface (Bath et al. 1974a) or transient hot spots in the disk (Bath 1973).

Since the whole disk appears to oscillate (Nather & Robinson 1974), it seems that the geometry of the disk should be investigated with an eye to the importance of reflection effects. The role of electron scattering in the disk is particularly relevant in connection with polarization of reflected light (Rees 1975).

3) Spectral properties

i) Continua

The most studied system is SS Cyg. It has been investigated in the soft X-ray (Rappaport et al. 1974), ultraviolet (Holm & Gallagher 1974), visual (e.g. Walker & Chincarini 1968) and infrared (Szkody 1974) spectral regions. Heise et al. (1975) have observed a number of dwarf novae in the soft X-ray region. Four systems were monitored at maximum. The only positive results were obtained for SS Cyg, which was detectable both at minimum and at maximum. Henry et al. (1975) observed U Gem and RX And in the far ultraviolet/soft X-ray region of the spectrum. Since no flux was detected, only upper limits on the radiation could be specified. Wu (1975)

presented results of ultraviolet studies of seven dwarf novae, some of which showed large departures from normal stellar flux distributions.

More generally, the CV-systems lie above the blackbody line in the U-B, B-V diagram at minimum, with continua resembling those of A or B-type stars at maximum (Mumford 1967). Hot spots lie below the blackbody line (Lortet 1969) and make a large contribution to the continuum radiation (e.g. Harwood 1973).

ii) Line spectra

These are discussed in depth by Glasby (1969). At minimum, asymmetric emission lines of the Balmer series, He I, He II and Ca II are observed. The lines are wide, sometimes doubled. The complex, (binary) phase dependent structure can be explained by the blending of contributions from the disk and the hot spot (Smak 1971, 1975). During the rise to maximum, wide, shallow absorption lines of H and He I dominate. At maximum emission cores sometimes occur. The extreme broadening could be due to either Doppler effects (in the disk) or to Stark interactions (on the dwarf surface) (Faulkner 1974).

Spectroscopically, novae appear to be hotter than dwarf novae at minimum. The observations of SS Cyg by Walker & Chincarini should be mentioned: at minimum, single lines of H, He I and a doubled Ca II-K line were seen in emission. Ultra-violet flares in the system affected the single lines only. At maximum all lines changed to absorption, velocity separation of the two Ca II components being larger in absorption than in emission.

4) Mass of the disk

From changes in the orbital periods of a number of systems, Smak (1972) deduced $M_d \gtrsim 10^{-6}\ M_\odot$. (See however, Pringle 1975. It should also be noted that Smak assumed that there is no mass loss from the binary system as a whole. This assumption might be doubtful, e.g. Robinson 1973.) Warner (1974) found $M_d \sim 10^{-5}\ M_\odot$.

Other characteristics of CV-systems

Some features which will be useful in making numerical model calculations:-

i) The masses of white dwarf components have been found generally to be near 1.2 $M_\odot$ (Warner 1973a). Chandrasekhar's mass-radius relationship then gives the stellar radius $R_s \sim 4 \times 10^8$ cm. This is in fair agreement with observational estimates $R_s \sim 10^9$ cm. (e.g. Warner 1974).

ii) The radius of the disk generally seems to be in the range $1.2 \times 10^{10} - 3 \times 10^{10}$ cm. (e.g. Harwood 1973, Warner 1974).

iii) Uncertainty exists as to accretion rates. Estimates of various authors (e.g. Krzeminsky & Smak (1971), Faulkner (1971) and others quoted in this introduction) seem to give $10^{16} \lesssim \frac{dM_r}{dt} \lesssim 10^{20}$ g sec^{-1} as the rate of mass loss by the red component. It is uncertain how much of the material eventually reaches the white dwarf surface (Robinson 1973, Osaki 1974).

Theoretical work on disk structures

Accretion onto white dwarfs has been discussed by Prendergast & Burbidge (1968) and De Gregoria (1974). Unfortunately the former paper only presented the results of numerical calculations and contained little theoretical information. The latter investigated time-dependent spherically symmetrical accretion.

Shakura (1973) and Shakura & Sunyaev (1973) made detailed calculations of disk accretion onto black holes and Pringle & Rees (1972) calculated the continuum spectrum of compact X-ray sources, using a simplified disk model. Lynden-Bell & Pringle (1974) studied the evolution of viscous disks. Of particular interest in their paper was the discussion of the region of interaction between the disk and central star. Lightman (1974a,b) described the time-dependent behaviour of accretion disks, using a variant of the viscosity law proposed by Shakura & Sunyaev. He found that regions in the disk where radiation pressure dominated over gas pressure were bound to be unstable. We shall examine these solutions in the steady state case.

Relativistic disks have been studied by Page & Thorne (1974), Thorne (1974) and Eardly & Lightman (1975). A model for the optically thin inner region of black hole disks has been constructed by Eardly et al. (1975).

Also of interest are papers by Lynden-Bell (1969) and Ter Haar (1950) on galactic disks and a solar disk respectively.

The purpose of this thesis is a discussion of the assumptions underlying disk models, in particular the viscosity law. Some comparisons of results with observations will also be made.

II. Derivation of equations

(a) Hydrodynamic and energy equations

In deriving these equations, turbulent motion will be assumed. The starting point is the well-known equations for laminar flow. Equations are set up in a cylindrical coordinate system with the origin at the centre of the primary and the z-axis perpendicular to the plane of symmetry of the disk.

We assume that:

i) Self-gravity of the disk is negligible

ii) The disk is axially symmetrical

iii) The disk is in a quasi-steady state

iv) Magnetodydrodynamic effects can be neglected

v) Influence of the secondary is negligible

vi) Mean vertical (z-directed) velocities are negligible.

In treating turbulent flows, it is convenient to define the mean value of a quantity x (density, temperature, etc.) as

$$\overline{x} = \frac{1}{2T} \int_{-T}^{T} x\,dt$$

where T is a time interval long compared with the quasi-period of the irregular turbulent fluctuations. The instantaneous value is denoted by

$$x = \overline{x} + x' \qquad (1.1.1)$$

where x' represents the fluctuating component, such that $\overline{x'} = o$.

1) Equation of continuity

$$\frac{1}{R}\frac{\partial}{\partial R}(\rho R V_r) + \frac{\partial}{\partial Z}(\rho V_z) = o \qquad (1.1.2)$$

Substitution of (1.1.1) and averaging yields

$$\frac{1}{R}\frac{\partial}{\partial R}\left[R(\bar{\rho}\bar{V}_r + \overline{\rho' V_r'})\right] + \frac{\partial}{\partial Z}\overline{\rho' V_z'} = o. \qquad (1.1.3)$$

In general the quantities $\overline{\rho' V_r'}$ and $\overline{\rho' V_z'}$ will not vanish, as fluctuations in density and velocity components are bound to be correlated.

In the remainder of this discussion we shall follow the example of Hinze (1959) (p.19) and assume that the mean quantities satisfy (1.1.3) approximately, i.e.

$$\frac{\partial}{\partial R}(R\bar{\rho}\bar{V}_r) \approx o \qquad (1.1.4)$$

2) Equations of motion

R-component:

$$\rho\left(V_r\frac{\partial V_r}{\partial R} - \frac{V_\theta^2}{R} + V_z\frac{\partial V_r}{\partial Z}\right) = -\frac{\partial P}{\partial R} - \left\{\frac{1}{R}\frac{\partial}{\partial R}(R\sigma_{rr}) - \frac{\sigma_{\theta\theta}}{R} + \frac{\partial}{\partial Z}\sigma_{rz}\right\} + \rho g_r$$

θ-component:

$$\rho\left(V_r\frac{\partial V_\theta}{\partial R} + \frac{V_r V_\theta}{R} + V_z\frac{\partial V_\theta}{\partial Z}\right) = -\left\{\frac{1}{R^2}\frac{\partial}{\partial R}(R^2\sigma_{r\theta}) + \frac{\partial}{\partial Z}\sigma_{\theta Z}\right\}$$

z-component:

$$\rho\left(V_r\frac{\partial V_z}{\partial R} + V_z\frac{\partial V_z}{\partial Z}\right) = -\frac{\partial P}{\partial Z} - \left\{\frac{1}{R}\frac{\partial}{\partial R}(R\sigma_{rz}) + \frac{\partial}{\partial Z}\right\}\sigma_{zz} + \rho g_z \qquad (1.1.5)$$

The stresses are given by

$$\sigma_{rr} = -2\eta \frac{\partial V_r}{\partial R} + \left(\frac{2}{3}\eta - \xi\right)\underset{\sim}{\nabla}.\underset{\sim}{V}$$

$$\sigma_{\theta\theta} = -2\eta \left(\frac{V_r}{R}\right) + \left(\frac{2}{3}\eta - \xi\right)\underset{\sim}{\nabla}.\underset{\sim}{V}$$

$$\sigma_{zz} = -2\eta \frac{\partial V_z}{\partial Z} + \left(\frac{2}{3}\eta - \xi\right)\underset{\sim}{\nabla}.\underset{\sim}{V} \qquad (1.1.6)$$

$$\sigma_{r\theta} = \sigma_{\theta r} = \eta R \frac{\partial}{\partial R}\left(\frac{V_\theta}{R}\right)$$

$$\sigma_{\theta z} = \sigma_{z\theta} = -\eta \frac{\partial V_\theta}{\partial Z}$$

$$\sigma_{rz} = \sigma_{zr} = -\eta\left(\frac{\partial V_z}{\partial R} + \frac{\partial V_r}{\partial Z}\right)$$

η and ξ are the first (dynamic) and second (bulk) coefficients of viscosity respectively, and $\underset{\sim}{\nabla}.\underset{\sim}{V} = \frac{1}{R}\frac{\partial}{\partial R}(RV_r) + \frac{\partial}{\partial Z}V_z$.

Proceeding as in the continuity equation and using (1.1.2)-(1.1.4),

$$\bar{\rho}\left(V_r \frac{\partial \bar{V}_r}{\partial R} \frac{\partial \bar{V}_\theta^2}{\partial R}\right) = -\frac{\bar{P}}{R} - \{\text{viscous terms}\}$$

$$-\frac{1}{R}\frac{\partial}{\partial R}R\{\bar{\rho}\,\overline{V_r'V_r'} + 2\bar{V}_r\,\overline{\rho'V_r'} + \overline{\rho'V_r'V_r'}\}$$

$$+\bar{\rho}g_r - \frac{\partial}{\partial Z}\{\overline{\rho V_r'V_z'} + \bar{V}_r\,\overline{\rho'V_z'} + \overline{\rho'V_r'V_z'}\}$$

$$+\frac{1}{R}\{\bar{\rho}\,\overline{V_\theta'V_\theta'} + 2\bar{V}_\theta\,\overline{\rho'V_\theta'} + \overline{\rho'V_\theta'V_\theta'}\}$$

$$\bar{\rho}\left(\bar{V}_r \frac{\partial \bar{V}_\theta}{\partial R} + \frac{\bar{V}_r \bar{V}_\theta}{R}\right) = -\frac{1}{R^2}\frac{\partial}{\partial R} R^2\{\bar{\rho}\,\overline{V'_r V'_\theta} + \bar{V}_r\,\overline{\rho' V'_\theta} + \bar{V}_\theta\,\overline{\rho' V'_r} + \overline{\rho' V'_r V'_\theta}\}$$

$$\{\text{viscous terms}\} - \frac{\partial}{\partial Z}\{\bar{\rho}\,\overline{V'_\theta V'_\theta} + \bar{V}_\theta\,\overline{\rho' V'_z} + \overline{\rho' V'_\theta V'_z}\}$$

and

$$\frac{\partial \bar{P}}{\partial Z} = -\frac{1}{R}\frac{\partial}{\partial R} R\{\bar{\rho}\,\overline{V'_r V'_z} + \bar{V}_r\,\overline{\rho' V' V'} + \overline{\rho' V'_r V_z}\}$$

$$-\frac{\partial}{\partial Z}\{\bar{\rho}\,\overline{V'_z V'_z} + \overline{\rho' V'_z V'_z}\} + \bar{\rho} g_z - \{\text{viscous terms}\}.$$

Comparison with the original equations (1.1.5) indicates that turbulent fluctuations cause additional "apparent" stresses given by:-

$$\left.\begin{aligned}
\tau_{rr} &= \bar{\rho}\,\overline{V'_r V'_r} + 2\bar{V}_r\,\overline{\rho' V'_r} + \overline{\rho' V'_r V'_r} \\
\tau_{\theta\theta} &= \bar{\rho}\,\overline{V'_\theta V'_\theta} + 2\bar{V}_\theta\,\overline{\rho' V'_\theta} + \overline{\rho' V'_\theta V'_\theta} \\
\tau_{zz} &= \bar{\rho}\,\overline{V'_z V'_z} + \overline{\rho' V'_z V'_z} \\
\tau_{r\theta} &= \bar{\rho}\,\overline{V'_r V'_\theta} + \bar{V}_r\,\overline{\rho' V'_\theta} + \bar{V}_\theta\,\overline{\rho' V'_r} + \overline{\rho' V'_r V'_\theta} \\
\tau_{\theta z} &= \bar{\rho}\,\overline{V'_\theta V'_z} + \bar{V}_\theta\,\overline{\rho' V'_z} + \overline{\rho' V'_\theta V'_z} \\
\tau_{rz} &= \bar{\rho}\,\overline{V'_r V'_z} + \bar{V}_r\,\overline{\rho' V'_z} + \overline{\rho' V'_r V'_z}
\end{aligned}\right\} \quad (1.1.7)$$

Experimentally it has been shown that the ordinary viscous terms are generally negligible compared to the virtual stresses (see eq. Schlichting p. 531). (Intuitively we can reason that momentum transport by macroscopic turbulent eddies is expected to dominate over molecular transport.) As a consequence, the equations for turbulent flow can be written in the form (1.1.5) with $\bar{V}_z = o$ with stresses given by (1.1.7).

3) Equation of state

Denoting the total pressure by p :-

$$p = p_r + p_g = \frac{1}{3} aT^4 + \frac{R}{\mu} \rho T \qquad (1.1.8)$$

Assuming μ to be insensitive to fluctuations and neglecting higher order terms in the fluctuating quantities, we get

$$\bar{p} = \frac{1}{3} a(\bar{T}^4 + 6\bar{T}^2 \overline{T'T'}) + \frac{R}{\mu} (\overline{\rho T} + \overline{\rho' T'}) \qquad (1.1.9)$$

4) Energy equation

In the case of laminar flow

$$\rho C_V \left(V_r \frac{T}{R} + V_z \frac{T}{Z}\right) = - \left\{\frac{1}{R} \frac{\partial}{\partial R} Rq_r^{(r)} + \frac{\partial}{\partial Z} q_z^{(r)}\right\}$$

$$- (4p_r + p_g) \left\{ \frac{1}{R} \frac{\partial}{\partial R} (RV_r) + \frac{\partial V_z}{\partial Z} \right\}$$

$$-\left\{\sigma_{rr} \frac{\partial V_r}{\partial R} + \sigma_{\theta\theta} \frac{V_r}{R} + \sigma_{zz} \frac{\partial V_z}{\partial Z} + \sigma_{r\theta} R \frac{\partial}{\partial R} \left(\frac{V_\theta}{R}\right) + \sigma_{rz} \left(\frac{\partial V_z}{\partial R} + \frac{\partial V_r}{\partial Z}\right) + \sigma_{\theta z} \frac{\partial V_\theta}{\partial Z} \right\}$$

(1.1.10)

Convection of bulk motion of the gas is represented by the LHS of the equation, $q_i^{(r)}$ denotes the radiative energy flux and the last two terms describe energy production by compression and viscous dissipation respectively.

For $q_i^{(r)}$ we shall use the diffusion approximation

$$q_r^{(r)} = -\frac{4}{3} ac \frac{T^3}{\bar{K}\rho} \frac{\partial T}{\partial R} \tag{1.1.11}$$

$$q_z^{(r)} = -\frac{4}{3} ac \frac{T^3}{\bar{K}\rho} \frac{\partial T}{\partial Z} , \tag{1.1.12}$$

$\bar{K}$ being a suitable mean absorption coefficient.

After some algebraic manipulation we find that (1.1.10) reduces to

$$\begin{aligned} \bar{\rho} C_v \bar{V}_r \frac{\partial \bar{T}}{\partial R} = & -\frac{1}{R}\frac{}{R} RC_v\{\bar{\rho}\,\overline{V_r'T'} + \bar{V}_r\,\overline{\rho'T'} + \overline{\rho'V_r'T'}\} \\ & - \frac{\partial}{\partial Z} C_v\{\bar{\rho}\,\overline{V_z'T'} + \bar{T}\,\overline{\rho'T_z'} + \overline{\rho'V_z'T'}\} \\ & - \frac{1}{R}\frac{\partial}{\partial R}(Rq_r^{(r)}) - \frac{\partial}{\partial Z} q_z^{(r)} - (4\bar{P}_r + \bar{P}_q)\frac{1}{R}\frac{\partial}{\partial R}(R\bar{V}_r) \\ & - \left\{\tau_{rr}\frac{\partial \bar{V}_r}{\partial R} + \tau_{\theta\theta}\frac{\bar{V}_r}{R} + \tau_{r\theta} R \frac{\partial}{\partial R}\left(\frac{\bar{V}_\theta}{R}\right) + \tau_{rz}\frac{\partial \bar{V}_r}{\partial Z} + \tau_{\theta z}\frac{\partial \bar{V}_\theta}{\partial Z}\right\} \end{aligned} \tag{1.1.13}$$

in the turbulent case. It has been assumed that

i) C_v and $q_i^{(r)}$ are insensitive to fluctuations. (Note that in the case of $q_i^{(r)}$, this is bound to be a bad approximation, due to the sensitive dependence of opacity on changes in temperature and density. Investigation of these effects are beyond the scope of this thesis.)

ii) Fluctuations in the compression term can be neglected compared to mean values

iii) Energy dissipation by stresses is negligible compared to turbulent dissipation

iv) Higher-order terms in turbulent dissipation are unimportant

v) C_v is a slowly varying function of position.

Comparison with (1.1.10) shows the appearance of turbulent energy fluxes

$$\left.\begin{aligned} q_r^{(t)} &= C_v \left\{ \bar{\rho}\, \overline{v_r' T'} + \bar{v}_r\, \overline{\rho' T'} + \bar{T}\, \overline{\rho' v_r'} + \overline{\rho' v_r' T'} \right\} \\ q_z^{(t)} &= C_v \left\{ \bar{\rho}\, \overline{v_z' T'} + \bar{T}\, \overline{\rho' v_z'} + \overline{\rho' v_z' T'} \right\} \end{aligned}\right\} \qquad (1.1.14)$$

(Note also that conduction and (free) convection have not been included. The former is not expected to play a role in disk structures. We shall return to the topic of convection when setting up a model.)

It would seem that the best approach to treatment the turbulent stresses and energy fluxes would be using experimental correlation measurements in (1.1.7), (1.1.14). Since, however, no such results seem to be available for hypersonic flow conditions (as is probably the case in CV-disks), the standard treatment in terms of a suitably defined turbulent "viscosity" has to be followed. In this regard the advice of Hinze (p. 21) will be adopted: the turbulent pressure is separated from the tangential stresses. Thus we let $\bar{P}_t = \bar{\rho} < \overline{U_i'^2} >$, where the brackets denote averaging over all i. (See also Batchelor 1955). (This is, strictly speaking, valid only if density fluctuations

are negligible, i.e. for incompressible flows.) For near-isotropic turbulence we then have

$$\overline{P}_t \approx \overline{\rho}\ \overline{U_i'^2}$$

and consequently

$$\tau_{rr} \approx \tau_{\theta\theta} \approx \tau_{zz} = \overline{P}_t \qquad (1.1.15)$$

(Note that in the present case where $\overline{V}_\theta \gg \overline{V}_r \gg \overline{V}_z$ is expected, it follows from (1.1.10) that the normal stresses could differ appreciably.)

In terms of an eddy viscosity the tangential stresses are given by

$$\tau_{r\theta} = -\eta_t\, R\, \frac{\partial}{\partial R}\left(\frac{\overline{V}_\theta}{R}\right) \qquad (1.1.16)$$

$$\tau_{rz} = -\eta_t\, \frac{\partial \overline{V}_r}{\partial Z} \qquad (1.1.17)$$

$$\tau_{\theta z} = -\eta_t\, \frac{\partial \overline{V}_\theta}{\partial Z} \qquad (1.1.18)$$

Similarly the turbulent energy fluxes can be written (Schlichting p. 660)

$$q_r^{(t)} = -C_p A_q\, \frac{\partial T}{\partial R} \qquad (1.1.19)$$

$$q_z^{(t)} = -C_p A_q\, \frac{\partial T}{\partial Z} \qquad (1.1.20)$$

where $A_q \equiv$ exchange coefficient for energy transfer by turbulence (see §II(c)).

The equations to be used in the turbulent case now read

$$\frac{\partial}{\partial R}\ R\rho V_r = o \qquad ((1.1.4))$$

$$\rho\left(V_r \frac{\partial V_r}{\partial R} - \frac{V_\theta^2}{R}\right) = -\frac{\partial}{\partial R}\ (P + P_t) - \frac{\partial}{\partial Z}\ \tau_{rz} + \rho g_r \qquad (1.1.21)$$

$$\rho\left(V_r \frac{\partial V_\theta}{\partial R} + \frac{V_r V_\theta}{R}\right) = -\left\{\frac{1}{R^2} \frac{\partial}{\partial R}\ (R^2 \tau_{r\theta}) + \frac{\partial}{\partial Z}\ \tau_{\theta z}\right\} \qquad (1.1.22)$$

$$\frac{\partial}{\partial Z}\ (P + P_t) = -\frac{1}{R} \frac{\partial}{\partial R}\ R\tau_{rz} + \rho g_z \qquad (1.1.23)$$

$$\left.\begin{aligned} \rho C_v V_r \frac{\partial T}{\partial R} = &-\left\{\frac{1}{R} \frac{\partial}{\partial R}\ R(q_r^{(r)} + q_r^{(t)}) + \frac{\partial}{\partial Z}\ (q_z^{(r)} + q_z^{(t)})\right\} \\ &- (4P_r + P_g + P_t) \frac{1}{R}\ \frac{\partial}{\partial R}\ RV_r \\ &- \left\{\tau_{r\theta}\ R \frac{\partial}{\partial R}\ \left(\frac{V_\theta}{R}\right) + \tau_{rz} \frac{\partial V_r}{\partial Z} + \tau_{\theta z} \frac{\partial V_\theta}{\partial Z}\right\} \end{aligned}\right\} \qquad (1.1.24)$$

where averaging bars have been dropped for convenience.

(b) Viscosity law

As has been pointed out by numerous authors, the appropriate form of the viscosity to be used is at present the greatest source of uncertainty in the theory of disk structures. We are faced with three possibilities: (a) laminar motion prevails, (b) the disk is unstable so that turbulent fluctuations are present, or (c) the disk is dynamically stable, but other effects (such as interaction between convection and orbital motions) cause turbulence. In addition, in cases (b) and (c),

it is not clear whether turbulent velocities would be supersonic. (This is particularly important as regards the role of turbulent pressure.)

A brief discussion of the viscosity laws for each case follows.

Case (a)

In a completely ionized gas, according to Mitchner & Kruger (1973) the viscosity due to an ion with mass m_i, charge z_i is given by

$$\eta_i = 0.406\ (4\pi\varepsilon_o)^2\ \frac{\sqrt{m_i}\ (kT)^{5/2}}{Z_i^4\ e^4\ \ell n\ \Lambda} \qquad (1.2.1)$$

(MKS units). Here e is the electronic charge, ε_o the permittivity of free space and

$$\Lambda \equiv \frac{\lambda_o}{b_o} = 1.24 \times 10^7\ \left(\frac{T^3}{N_e}\right)^{\frac{1}{2}} ,$$

λ_o being the Debye length, $\bar{b}_o$ the impact parameter for a 90^o scattering of an average particle in the plasma, and N_e the electron density.

The ratio of electronic to ionic viscosity is approximately

$$\frac{\eta_e}{\eta_i} \sim \frac{N_e}{N_i}\ \left(\frac{M_e}{M_i}\right)^{\frac{1}{2}}$$

so that η_e is usually negligible.

The second coefficient of viscosity manifests itself in

situations where the energy equilibrium between translational and internal degrees of freedom of a molecule has been perturbed (such as in sound-wave propagation). (Chapman & Cowling (1960), Schaaf (1963)). This viscosity can probably be disregarded in the present context.

We shall have occasion to use the mean free path approximation

$$\eta_\ell \sim V_T \bar{\ell}_T \rho \sim V_s \bar{\ell}_T \rho \qquad (1.2.2)$$

(since, by the equipartition theorem, $\bar{V}_T \sim V_s$).

Case (b)

If we postulate the validity of the hydrodynamic approach to the problem, it is possible to show that the Reynolds number of the disk should be fairly large:

$$R_c \equiv \frac{\bar{\rho}\bar{V}_o\lambda}{\bar{\eta}_\ell}$$

where averages are taken over the entire disk and λ is a characteristic dimension.

$$R_c \sim \left(\frac{\bar{V}_o}{\bar{V}_s}\right)\left(\frac{\lambda}{\bar{\ell}_T}\right) = \bar{M}\left(\frac{\lambda}{\bar{\ell}_T}\right) ,$$

$\bar{M}$ = mean Mach number of the flow. Since $\frac{\lambda}{\bar{\ell}_T} \gtrsim 10^2$ (say) must hold for the hydrodynamic approach to be applicable, $Re \gtrsim 100\,\bar{M}$. Now if we assume a mean Keplerian velocity $\bar{V}_o \sim 10^8$ cm s^{-1}, mean temperature between 10^3 and 10^5 ^oK,

$30 \lesssim \bar{M} \lesssim 300$ (i.e. hypersonic flow). Thus $R_e \gtrsim 10^3 - 10^4$, and since turbulent instabilities ordinarily ensues at these values of R_e in laboratory situations, it is usually assumed that the disk is unstable. The viscosity laws applicable to fully developed turbulent flows (i.e. very high R_e) are those of Chandrasekhar & Ter Haar, and Von Kármán.

Ter Haar (1950), in a model for a solar disk, made use of turbulence theory developed by Heisenberg to derive $V_t \approx \frac{1}{\sqrt{3}} V_\theta$, $\ell = 0.6\ R$ for the mean turbulent velocity and largest eddy size respectively. (The numerical factor 0.6 was found by comparing theoretical results with Bode's law.) This would give

$$\eta_t \approx 0.3\ \rho V_\theta R \tag{1.2.4}$$

The semi-empirical Von Kármán law reads

$$\eta_t = \rho K^2 \left| \frac{(\tfrac{1}{2}\Delta_{ij}\Delta_{ji})^{3/2}}{\tfrac{1}{2}\Omega_{ij}\Omega_{ij}} \right|$$

in the usual tensor notation (Von Kármán 1956). Here $K \approx 0.4$, a "universal" constant, and

$$\Delta_{ij} \equiv \frac{\partial V_i}{\partial X_j} + \frac{\partial V_j}{\partial X_i}$$

$$\Omega_{ij} \equiv \frac{\partial \omega_i}{\partial X_j} + \frac{\partial \omega_j}{\partial X_i}$$

$$\underset{\sim}{\omega} \equiv \underset{\sim}{\nabla} \times \underset{\sim}{V}$$

Setting $V_z = o$ and assuming $V_r \ll V_\theta = \sqrt{\frac{GM}{R}}$ (i.e. Keplerian motion in a thin disk), we find

$$\eta_t = 6K^2 \rho R V_\theta \approx \rho R V_\theta \qquad (1.2.5)$$

Note the similarity between (1.2.4) and (1.2.5).

Both these laws were derived for subsonic, incompressible flows. We have seen, however, that flow in the disk is probably highly supersonic. Von Weizsäcker (1951) has suggested changes to Heisenberg's theory for application to compressible fluids, while more recently Shakura & Sunyaev (1973) have proposed a different approach based on intuitive ideas.

Von Weizsäcker's interpretation of a theory for compressible turbulence (originally developed by Von Hoerner) has recently been revived in a cosmogonical context (see Harrison (1973) for numerous references). We shall here follow the reasoning of Dellaporta & Lucchin (1972,1973).

It is well known that in turbulent flows a hierarchy of eddy sizes and corresponding velocities is obtained, the largest eddies being of the order of the system dimensions. In the case of fully developed turbulence the relation between eddy size and velocity is given by the Kolmogorov spectrum (see e.g. Landau & Lifschitz 1959, Chandrasekhar 1949)

$$V_\lambda \sim \lambda^{1/3} , \qquad (1.2.6)$$

where $\lambda \equiv$ eddy size, $V_\lambda \equiv$ corresponding eddy velocity. For supersonic flows, part of this spectrum will lie in the supersonic range. Dallaporta & Lucchin suggest that density fluctuations associated with the supersonic part of the turbulence spectrum will be appreciable and that such fluctuations are indeed necessary for the formation of galaxies from

a turbulent primeval gas. Following, Von Weizsäcker, they assume

$$\frac{\rho_{\lambda_1}}{\rho_{\lambda_2}} = \left(\frac{\lambda_2}{\lambda_1}\right)^{3k} \qquad (1.2.7)$$

where subscripts 1 and 2 refer to eddies of extent λ_1 and λ_2 respectively. The compressibility index k lies between o and 1, such that k = o for incompressible flow, k = 1 for complete compressibility. (Von Weizsäcker quotes $k \approx 0.07$ for the Orion nebula while Dallaporta & Lucchin find $k \sim 0.5 - 0.6$ for galaxy formation.) The assumption (1.2.7) modifies (1.2.6) to

$$V_\lambda \sim \lambda^{k+1/3}$$

for $V_\lambda > V_s$. The subsonic spectrum remains unaltered as compressibility is less important. Note that no account of shock waves is necessary in this theory. Von Weizsäcker assumes that the wave fronts will be destroyed by large-amplitude density variations.

Shakura & Sunyaev (SS) on the other hand, believe that shock formation will occur, inhibiting supersonic eddy velocities. Rapid dissipation of this energy will furthermore raise the sound velocity, shifting the supersonic spectrum towards the subsonic. (See also Cox & Giuli (CG) p. 293.) Similarly Lighthill (1953,1955) proposed that supersonic gas flow would be characterized by a situation where eddies and shock waves propagate randomly. According to him, interaction between shock waves could play an important part in the structure of this turbulence.

In summary: it seems that in the case of supersonic flows, the results of Ter Haar and Von Kármán should be modified by either considering the effects of density variations on the supersonic spectrum of by deleting the supersonic part and taking proper account of the shock waves.

Case (c)

As remarked by Pringle (1973), the disk might be dynamically stable. We will discuss this possibility very briefly.

Turbulence is caused by the propagation and amplification of disturbances in the fluid, so that a study of the behaviour of perturbations must be made. This has been done for an incompressible fluid in a situation similar to that of the disk (Chandrasekhar 1961). It is found that motion will be stable if Rayleigh's criterion

$$\phi(R) = \frac{d}{dR} (RV_\theta)^2 > o$$

is satisfied. For Keplerian motion $V_\theta \approx \sqrt{\frac{GM}{R}}$, $\phi(R) = GM$ so that stable flow is expected. (This argument has been used by Batchelor (1958) in support of laminar motion of cosmic gas in stellar gravitational fields.) Recently Stewart (1975) has analyzed stability requirements in disks in detail: assuming compressible, inviscid fluid motion be found that most non-axisymmetrical perturbations lead to secular instability. Axisymmetric stability is described by the Rayleigh and Schwarzschild (convective) criteria.

It must be noted that even in dynamically stable disks, some form of turbulence might be present due to the interaction

between fluid elements travelling in different directions, e.g. orbital and convective motions.

We conclude this section by mentioning a few other viscosity laws. Batchelor (1955) examined turbulence in a gaseous disk and concluded that the most probable equilibrium configuration (under the action of self-gravity) would be characterized by the near equality of gas and turbulent pressures, i,e, $V_t \approx V_s$. This is a special case of the SS-law $V_t = \alpha V_s$ ($\alpha \lesssim 1$). Lightman (1974a,b) used $\tau_{r\theta} = \alpha(p_r+p_g)$, $\alpha \lesssim 1$ for the tangential stress. This normally reduces to the law of SS. LBP suggested that the turbulent viscosity is determined by

$$Re_{eff} = \rho \frac{V_{\theta_s} R_s}{\eta_t} = Re_c \quad ;$$

here Re_{eff} effective Reynolds number, V_{θ_s} Keplerian velocity at $R = R_s$, $Re_c \equiv$ critical Reynolds number for transition from laminar to turbulent flow. By analogy with laboratory results, they suggest $Re_c \approx 10^3$; it is reasoned that smaller values of Re_{eff} would cause a tendency to increased turbulence. (This is perhaps doubtful. It also seems unlikely that turbulent viscosity should be independent of the velocity distribution in the disk.)

(c) Other useful relations

For the model to be constructed we shall adopt the SS viscosity law

$$\eta_t = \alpha \rho V_s Z_o \; . \qquad (1.3.1)$$

α is a dimensionless function of position and Z_o a suitable mixing length, here equated to the vertical length scale ($\approx$ vertical scale height) in the disk. The restriction $\alpha \leq 1$ is dropped so that the consequences of allowing supersonic eddy velocities can be studied.

For consistency we should have $\eta_t \gg \eta_\ell$, or by (1.2.2) $\frac{\alpha Z_o}{\bar{\ell}_T} \gg 1$. If we use the approximation $\bar{\ell}_T \sim 10^{-19}\ T^2/\rho$ cm (valid for a fully ionized gas; Allen 1973 (pp.49,50)). then the condition can be written

$$\frac{\alpha Z_o \rho}{T^2} \gg 10^{-19} \tag{1.3.2}$$

According to Landau & Lifschitz (1959) a general expression for sound velocity ($\gamma = 5/3$, $\mu = 1$) is

$$\begin{aligned} V_s^2 &= \frac{5}{3}\frac{kT}{M_p}\left\{1 + \frac{32}{45}\ \frac{(aM_pT^3)^2}{k^2\rho\left(\rho + 8/5\ \frac{aM_pT^3}{k}\right)}\right\} \\ &\approx \frac{5}{3}\frac{kT}{M_p}\left\{1 + \frac{32}{5}\ \frac{P_r^2}{P_g^2\left(1 + 8\ \frac{P_r}{P_g}\right)}\right\} \end{aligned} \tag{1.3.3}$$

(see (1.1.8); $R = \frac{k}{M_p}$). This can be shown to reduce to

$$V_s^2 \sim P_g/\rho \qquad (P_g \gg P_r) \tag{1.3.4}$$

$$V_s^2 \sim P_r/\rho \qquad (P_r \gg P_g) \tag{1.3.5}$$

By allowing supersonic eddy velocities ($\alpha > 1$) we bring into play a third pressure (Batchelor 1955):-

$$P_t = {}^1/_3 \rho V_t^2 \sim \alpha^2 \rho V_s \qquad (1.3.6)$$

(see also Ter Haar 1950). Comparison with (7.3.4), (1.3.5) shows that P_t dominates if $\alpha \gg 1$. This has some interesting consequences in the treatment of turbulent energy transfer.

From experimental measurements it is known that the exchange coefficient for energy transport in turbulent flow (cf. (1.1.19), (1.1.20)) obeys $\frac{A_q}{\eta_t} \sim 1$ (Schlichting pp.660,661), so that

$$q_i^{(t)} \approx - C_p \eta_t \frac{\partial T}{\partial X_i} = - \alpha \rho V_s Z_o C_p \frac{\partial T}{\partial X_i} \qquad (1.3.7)$$

Now according to CG (p. 218)

$$C_v = \frac{R}{\mu(\gamma-1)} \left\{ \frac{12(1-\beta)(\gamma-1) + \beta}{\beta} \right\} \qquad (1.3.8)$$

where $\beta \equiv P_g/P \quad P_g/(P_r+P_g)$. (For later use we also note that

$$\frac{C_p}{C_v} = 1 + \frac{(4-3\beta)^2(\gamma-1)}{12\beta(1-\beta)(\gamma-1) + \beta^2} \qquad (1.3.9)$$

which reduces to $\frac{C_p}{C_v} = \gamma$ if $\beta = 1$, i.e. P_r negligible.) What happens when turbulent pressure becomes important? We may write (CG p. 213)

$$\frac{C_p}{C_v} = 1 + \frac{P}{\rho E} \qquad (1.3.10)$$

provided the equation of state is of the ideal gas form $P = \text{const. } \rho T$. In the case of dominant turbulent pressure, $P_g \gg P_r$ we have $P_t \approx \alpha^2 P_g$ ((1.3.6), (1.3.4)) which satisfies

this condition. Also, the turbulent energy per unit mass is $E_t = V_t^2 = \alpha^2 V_s^2 \approx \alpha^2 E_g$, so that $\frac{C_{pt}}{C_{vt}} = 1 + \frac{P_t}{\rho E_t} \approx 1 + \frac{P_g}{\rho E_g} = \gamma$.

We proceed to derive an explicit expression for C_{pt} :

In general $C_p - C_v = \frac{P}{\rho T} \frac{\chi_T^2}{\chi_\rho}$ (CG p. 210), when $\chi_T \equiv \frac{\partial \ell n P}{\partial \ell n T}\Big)_\rho$, and $\chi_\rho \equiv \frac{\partial \ell n P}{\partial \ell n \rho}\Big)_T$. For our case $C_{pt} - C_{vt} \approx \alpha^2 \frac{P_g}{\rho T} = \alpha^2 \frac{R}{\mu}$, so that

$$C_{pt} \approx \alpha^2 C_{pg} \tag{1.3.11}$$

Similarly, if $P_t \gg P_r \gg P_g$,CG's analysis (pp. 217 ff) can be repeated using the relations

$$P \approx (1 + \alpha^2) \frac{aT^4}{3} + \frac{R}{\mu} \rho T$$

$$E \approx (1 + \alpha^2) \frac{aT^4}{\rho} + \frac{RT}{\mu(\gamma-1)}$$

for the total pressure and energy/unit mass respectively. (1.3.8), (1.3.9) are again obtained, but now $\beta = P_g/(P_r+P_g+P_t) \approx P_g/(1 + \alpha^2)P_r + P_g$. If $\beta \ll 1$,

$$C_v = \frac{4aT^3}{\rho} (1 + \alpha^2) \tag{1.3.12}$$

$$\frac{C_p}{C_v} \approx 1 + \frac{4}{3\beta} = 1 + \frac{4}{3} (1 + \alpha^2) \frac{P_r}{P_g} \tag{1.3.13}$$

It follows that the efficiency of turbulent heat transfer is increased in the supersonic region of the eddy velocity spectrum not only by the higher velocities, but also by the

increased specific heats.

It should be noted that this increase in heat capacity is a consequence of the assumed viscosity law. Thus for the Ter Haar and Von Kármán viscosities (V_t independent of V_s and therefore of T), $\chi_T = o$ so that $C_{pt} = C_{vt}$. Also E_t is independent of T so that $C_{pt} = C_{vt} = o$.

Before proceeding to the model, we mention the criterion for convective stability (Chandrasekhar 1939 p. 57):

$$\frac{d\ell nP}{d\ell nT} > \frac{\Gamma_2}{\Gamma_2 - 1} \tag{1.3.14}$$

Hence

$$\frac{\Gamma_2}{\Gamma_2 - 1} \equiv \frac{12\beta(1-\beta)(\gamma-1) + \beta^2 + (4-3\beta)^2(\gamma-1)}{(4-3\beta)(\gamma-1)} \tag{1.3.15}$$

If $P_g \gg P_r$, (1.3.12) reduces to

$$\frac{d\ell nP}{d\ell nT} > \frac{\gamma}{\gamma - 1} \tag{1.3.16}$$

The influence of ionization processes on specific heats, the gas pressure and convection will not be considered here.

III. Model

The aim of this section will be the derivation of dimensionless equations describing the vertical structure of the disk at each radial position. Equations linking scale factors and boundary values (at different R-values) are also to be found. Although we assume the validity of the SS viscosity law, no restrictions will be placed on the parameter α so that other laws can be represented by a suitable choice of its functional dependence.

The vertical length scale is found as follows (see also SS, Lynden-Bell 1969): Using (1.3.4)-(1.3.6) we write the equation of state $P \approx (1 + \alpha^2)\rho V_s^2$. Assuming α, V_s independent of Z and neglecting τ_{rz} in (1.1.23), this last equation reduces to

$$(1 + \alpha^2) V_s^2 \frac{\partial \rho}{\partial Z} \approx \rho g_z \approx - \frac{GM}{R^3} Z\rho$$

for a thin disk (i.e. $Z \ll R$ everywhere in the disk.) This can be integrated to give

$$\rho(R,Z) = \rho_o(R) \exp - \left(\frac{Z}{Z_o}\right)^2$$

where $Z_o = \sqrt{2(1+\alpha^2)} V_s / \sqrt{\frac{GM}{R^3}}$ is the vertical scale height. In general α and V_s are expected to vary with Z : Z_o will therefore be defined in terms of the values at Z = o. We introduce the abbreviation $\omega \equiv \sqrt{\frac{GM}{R^3}}$, so that

$$Z_o = \sqrt{2(1 + \alpha^2)} \frac{V_{s_o}}{\omega} \qquad (2.1.1)$$

The conditions for V_θ to reduce to the Keplerian θ-velocity

$$V_{\theta K} = R\sqrt{\frac{GM}{S^3}} = R\omega_K \,, \qquad (2.1.2)$$

$S = \sqrt{R^2 + Z^2}$, can now be found. Examination of (1.1.21) reveals that the conditions to be fulfilled are

$$\left|\frac{\partial}{\partial Z}\,\tau_{rz}\right| \ll \rho|g_r| \,, \quad \left|\frac{\partial}{\partial R}\,(P+P_t)\right| \ll \rho|g_r|$$

and

$$\left|V_r\,\frac{\partial V_r}{\partial R}\right| \ll \rho|g_r| \,.$$

Using (1.1.17) leads to the order of magnitude estimate

$\eta_t \dfrac{|V_r|}{Z_o^2} \ll \rho|g_r| = \rho R\omega_K^2$ for the first requirement. For the viscosity

$$\eta_t = \alpha\rho V_s Z_o \qquad (2.1.3)$$

we have

$$\frac{\alpha|V_r|}{\sqrt{1+\alpha^2}\;V\theta K} \ll \frac{\omega_K}{\omega} \sim 1$$

The second condition gives $(1 + \alpha^2)V_s^2 \ll R|g_r| = V_{\theta K}^2$ while the last reduces to $|V_r| \ll V_{\theta K}$; the last condition is more stringent than the first for $\alpha \ll 1$ and equivalent to it for large α. Provided then that

$$\text{(i)} \qquad \frac{|V_r|}{|V_{\theta K}|} \ll 1$$

$$\text{(ii)} \qquad (1 + \alpha^2)\left(\frac{V_s}{V_{\theta K}}\right)^2 \ll 1$$

we have $V_\theta \approx V_{\theta K}$.

Also, by (1.1.16), (1.1.18)

$$\frac{\tau_{r\theta}}{\tau_{\theta z}} \approx R \frac{\frac{\partial \omega_K}{\partial R}}{\frac{\partial V_\theta}{\partial Z}} = \frac{\frac{\partial S}{\partial R}}{\frac{\partial S}{\partial Z}} = \frac{R}{Z}$$

We shall assume (iii) $Z/R \ll 1$ everywhere in the disk, so that $\tau_{r\theta} \gg \tau_{\theta z}$ and consequently (1.1.22) reduces to

$$\rho V_r \frac{\partial}{\partial R} (RV_\theta) = -\frac{1}{R} \frac{\partial}{\partial R} (R^2 \tau_{r\theta})$$

Here

$$\tau_{r\theta} = -\eta_t R \frac{\partial \omega_K}{\partial R} \approx \frac{3}{2} \alpha \rho V_s Z_o \omega \qquad (2.1.4)$$

in the thin-disk approximation where $V_\theta \approx R\omega$. Thus

$$\rho V_r R \frac{d}{dR} (RV_\theta) = \frac{3}{2} \frac{\partial}{\partial R} R^2 (\alpha \rho V_s Z_o \omega) \qquad (2.1.5)$$

(1.1.23) can also be written in a simpler form since

$$\left| \frac{1}{R} \frac{\frac{\partial}{\partial R} (R\tau_{rz})}{\frac{\partial P}{\partial Z}} \right| \sim \frac{|\tau_{rz}|/R}{(1+\bar{\alpha}^2)\rho V_s^2/Z_o} \sim \frac{\eta_t |V_r|}{(1+\alpha^2)\rho V_s^2 R} \qquad (\because (1.1.17))$$

$$= \frac{\alpha}{1+\alpha^2} \frac{|V_r| Z_o}{R V_s} \sim \frac{\alpha}{\sqrt{1+\alpha^2}} \frac{|V_r|}{V_o} .$$

Provided assumption (i) holds, we then have

$$\frac{\partial}{\partial Z} (P+P_t) \approx \rho g_z \qquad (2.1.6)$$

In order to proceed, it is necessary to make some assumption about the variation of V_r with Z. Intuitively we expect V_r to be determined by the viscosity, so that

$$V_r(R,Z) = V_r(R,O)\ \frac{\eta_t(R,Z)}{\eta_t(R,O)} = V_{r_o}\ \frac{\eta_t}{\eta_{t_o}}$$

seems a reasonable choice. Introducing the dimensionless variables

$$U = \frac{\rho(R,Z)}{\rho(R,O)} = \frac{\rho}{\rho_o}\ ,\ y \equiv \frac{Z}{Z_o}\ ,\ V \equiv \frac{T}{T_o}\ ,\ \alpha' \equiv \frac{\alpha}{\alpha_o}\ ;$$

$V_r = V_{r_o}\ \alpha' U V^{\frac{1}{2}}$ if $P_g \gg P_r$. We shall retain this form of V_r; in cases where $P_r \gg P_g$, α' can be chosen to give the proper functional dependence of V_r on U and V.

In order to describe the expected reduction in turbulent mixing length with increasing y, we will replace Z_o by $Z_o\beta(y)$, where β is to be adjusted at each new density scale height. Since α', U, V, β all presumably decrease with increasing Z, V_r will be neglected for $|Z| > \beta_1 Z_o$, i.e. $|Z|$ larger than the first scale height above Z = o.

Using these postulates the continuity equation (1.1.4) can be interpreted to give

$$\int_{-\infty}^{+\infty} \frac{\partial}{\partial R}\ (\rho R V_r) = \frac{d}{dR}\left[\int_{-\beta_1 Z_o}^{\beta_1 Z_o} \rho R V_r dz\right] - 2(\rho R V_r)_{\beta_1 Z_o}\ \frac{d}{dR}\ (\beta_1 Z_o)$$

$$\approx \frac{d}{dR}\ R Z_o \rho_o\ V_{r_o}\ \beta_1 \int_{-\beta_1}^{\beta_1} \alpha^1 U^2 V^{\frac{1}{2}} dy$$

$$= \frac{d}{dR}\ (R\rho_o V_{r_o} Z_o X_1)\ ,$$

where $X_1 \equiv \beta_1 \int_{-\beta_1}^{\beta_1} \alpha^1 U^2 V^{\frac{1}{2}}\, dy$. Clearly

$$\rho_o Z_o V_{r_o} X_1 R = \frac{\dot{M}}{2\pi} \tag{2.1.7}$$

where $\dot{M}$ is the accretion rate onto the star.

Returning to (2.1.5), integration over $(-\beta_1 Z_o, \beta_1 Z_o)$ gives

$$\frac{\dot{M}}{2\pi} \frac{d}{dR} (RV_\theta) = \frac{3}{2} \frac{d}{dR} R^2 (\alpha_o \rho_o V_{s_o} X_2 Z_o^2 \omega) - 3\beta_1 R^2 Z_o \omega (\alpha \rho V_s)_{\beta_1 Z_o} \frac{d}{dR} (\beta_1 Z_o)$$

$$\simeq \frac{3}{2} \frac{d}{dR} R^2 (\alpha_o \rho_o V_{s_o} X_2 Z_o^2 \omega)$$

where $X_2 \equiv \beta_1 \int_{-\beta_1}^{\beta_1} \alpha^1 U V^{\frac{1}{2}}\, dy$. Integration with respect to R yields

$$\frac{\dot{M}}{2\pi} RV_\theta = R^2 T_{r\theta} + C \tag{2.1.8}$$

with C ≡ const., $T_{r\theta} \equiv 3/2\ \alpha_o \rho_o V_{s_o} X_2 Z_o^2 \omega = \int_{-\beta_1 Z_o}^{\beta_1 Z_o} \tau_{r\hat{\theta}}\, dz$.

$T_{r\theta}$ is approximately equal to the stress between adjacent annuli of matter in the disk.

Consider now the situation near the stellar surface: if we assume that the rotational velocity ω_s (at the surface) is less than the break-up value $\sqrt{\frac{GM}{R_s^3}}$, then the angular velocity in the disk will adapt from the Keplerian form to the lesser value ω_s somewhere close to the star (i.e. in the viscous

boundary layer). This implies that ω reaches a maximum at some $R = R_m$; at this radial position $\frac{d\omega}{dR} = o$ and consequently $\tau_{r\theta}(R_m) = o$, $T_{r\theta}(R_m) \approx o$. R_m is expected to be very near R_s ; we follow LBP in setting $R_m = R_s$, $V_\theta(R_m) \approx V_{\theta K}(R_m) \approx V_{\theta K}(R_s)$ $= \sqrt{\frac{GM}{R_s^3}}$.

The constant in (2.1.8) can now be determined ($C = \frac{\dot{M}}{2\pi}\sqrt{gMR_s}$) and after rearranging we find

$$T_{r\theta} = \frac{\dot{M}}{2\pi} \omega(1-r^{-\frac{1}{2}}) , \qquad (2.1.9)$$

$r \equiv R/R_s$.

The surface density of the "core" $|Z| \lesssim \beta_1 Z_o$ of the disk is defined by

$$U_o \equiv \int_{\beta_1}^{\beta_1} \rho dz = \rho_o Z_o X_3 \qquad (2.1.10)$$

with $X_3 \equiv \int_{-\beta_1}^{\beta_1} U dy$. Model calculations (Pringle 1974,SS) show that most of the matter in the disk resides in the core, so that the disk mass is approximately

$$M_d \approx 2\pi \int_{R_s}^{R_d} U_o R dR \qquad (2.1.11)$$

In terms of the surface density (2.1.9) becomes

$$\frac{3}{2} U_o \alpha_o V_{s_o} Z_o \omega \left(\frac{X_2}{X_3}\right) = \frac{\dot{M}}{2\pi} \omega (1-r^{\frac{1}{2}})$$

or

$$3\alpha_o\sqrt{2(1+\alpha_o^2)}\;\; U_o V_{s_o}^2 \left(\frac{X_2}{X_3}\right) = \frac{M}{\pi}\;\omega(1-r^{-\frac{1}{2}}) \qquad (2.1.12)$$

($\because$ (2.1.1)).

The energy equation (1.1.24) can now be simplified. We have

$$\frac{\tau_{\theta z}\;\frac{\partial V_\theta}{\partial Z}}{\tau_{r\theta}\;R\,\frac{\partial}{\partial R}\left(\frac{V_\theta}{R}\right)} = \left(\frac{Z}{R}\right)^2 \ll 1$$

if $V_\theta = V_{\theta K}$ and assumption (iii) holds. Also

$$\frac{\tau_{rz}\;\frac{\partial V_r}{\partial Z}}{\tau_{r\theta}\;R\,\frac{\partial}{\partial R}\left(\frac{V_\theta}{R}\right)} \sim \frac{\left(\frac{V_r}{Z_o}\right)^2}{\omega^2} \sim \frac{1}{1+\alpha^2}\left(\frac{V_r}{V_s}\right)^2$$

From (2.1.7), (2.1.12) it can be shown that

$$\frac{V_r}{V_s} \sim \frac{\alpha\sqrt{1+\alpha^2}}{(1-r^{-\frac{1}{2}})}\left(\frac{V_s}{V_\theta}\right) \qquad (2.1.13)$$

so that, subject to the validity of assumption (ii), the heat production of the $\tau_{r\theta}$-stress is negligible excepting the immediate vicinity of the star. We shall not attempt to treat this viscous boundary layer here.

Concerning the importance of compressive heating as compared to viscous dissipation by the tangential stress:

$$\frac{(4P_r+P_g+P_t)\;\frac{1}{R}\frac{\partial}{\partial R}(RV_r)}{\tau_{r\theta}\;R\,\frac{\partial}{\partial R}\left(\frac{V_\theta}{R}\right)} \sim \frac{(1+\alpha^2)\;\frac{V_r}{R}\;\rho V_s^2}{\alpha\rho Z_o V_s \omega^2} \sim \frac{\sqrt{1+\alpha^2}}{\alpha}\;\frac{V_r}{V_\theta}\;.$$

For $\alpha > 1$, the pressure term is negligible if assumption (i) is satisfied. For $\alpha < 1$, we shall strengthen assumption (i) to $\left|\frac{V_r}{V_\theta}\right| \ll \alpha$ and neglect compressive heating in this case as well.

(1.1.24) reduces to

$$\rho C_v V_r \frac{\partial T}{\partial R} = \frac{1}{R}\frac{\partial}{\partial R} R \left(q_r^{(t)}+q_r^{(r)}\right) + \frac{\partial}{\partial Z}\left(q_z^{(t)}+q_z^{(r)}\right) + \tau_{r\theta} R \frac{d}{dR}\left(\frac{V_\theta}{R}\right)$$

We note, however, that

$$\frac{\rho C_v V_r \frac{\partial T}{\partial R}}{\frac{\partial}{\partial Z} q_z^{(t)}} \sim \frac{\rho C_v V_r Z_o^2}{\eta_t C_p R} \sim \frac{C_v}{C_p}\frac{V_r}{\alpha V_s}\frac{Z_o}{R} \sim \frac{C_v}{C_p}\frac{\sqrt{1+\alpha^2}}{\alpha}\frac{V_r}{V_\theta} .$$

Since $\frac{C_v}{C_p} \sim 1$ if $P_g \gg P_r$, $\frac{C_v}{C_p} \to 0$ if $P_r \gg P_g$, the forced-convection term is negligible if the modified form of assumption (i) holds. Assumption (iii) implies that the radial flux divergence terms are negligible compared to the vertical terms. (In the case of radiative transfer this comes about because the greater radial length scale implies a larger optical depth to be traversed by the flux; consequently radiation prefers to flow in the z-direction. Radial turbulent flux divergence is small because the turbulent mixing is effective only over distances $\sim Z_o \ll R$.)

The final form of the energy equation is

$$\frac{\partial}{\partial Z}\left[q_z^{(t)} + q_z^{(r)}\right] \approx - \tau_{r\theta} R \frac{d\omega}{dR} = \frac{3}{2} \tau_{r\theta}\omega .$$

$$\therefore \quad q_z^{(t)}(z) + q_z^{(r)}(z) = \frac{3}{2}\omega \int_o^z \tau_{r\theta} dz.$$

(2.1.4), (2.1.12) can be used to write this in the form

$$q_z^{(t)}(z)+q_z^{(r)}(z) = \frac{3}{4\pi}\frac{\dot{M}\omega^2}{X_2}(1-r^{\frac{1}{2}})\int_o^y \beta(y)\alpha^1 UV^{\frac{1}{2}}dy$$

$$= \frac{2}{X_2} Q \int_o^y \beta(y)\alpha^1 UV^{\frac{1}{2}}dy \qquad (2.1.14)$$

where $Q \equiv \frac{3}{8\pi}\dot{M}\omega^2(1-r^{-\frac{1}{2}})$. We note that $q_z^{(t)}(Z_o) = Q$. As most of the energy is produced in the region $|Z| < \beta_1 Z_o$ in the disk,

$$L_d \approx 4\pi\int_{R_s}^{R_d} QRdR = \frac{3}{2}\frac{\dot{M}GM}{R_s}\int_1^{r_d}(r^{-2} - r^{-5/2})dr$$

$$\therefore\quad L_d \approx \frac{1}{2}\frac{\dot{M}GM}{R_s}(1 - 3r_d^{-1} + 2r_d^{-3/2}) \qquad (2.1.16)$$

However, the rate of gravitational energy release is approximately

$$L_{tot} \approx \left[\frac{1}{2}\frac{\dot{M}GM}{R_d} - \frac{\dot{M}GM}{R_d}\right] - \left[\frac{1}{2}\dot{M}(R_s\omega_s)^2 - \frac{\dot{M}GM}{R_s}\right]$$

$$= \frac{1}{2}\frac{\dot{M}GM}{R_s}\left[(2-\varepsilon) - \frac{1}{r_d}\right] \qquad (2.1.17)$$

with $\varepsilon \equiv \frac{\omega_s}{\sqrt{\frac{GM}{R_s}}}$. Thus

$$L_{st} \approx L_{tot} - L_d \approx \frac{1}{2}\frac{\dot{M}GM}{R_s}(1-\varepsilon+ 2r_d^{-1} - 2r_d^{-3/2}) \qquad (2.1.18)$$

is the rate of energy release at the stellar surface.

To facilitate numerical solution of (2.1.6), (2.1.14) these will be written in dimensionless form. The equation of state is

$$P + P_t \approx \frac{k}{M_p}\ \rho T + \frac{1}{3}\ aT^4 \ + \ \alpha^2 \rho V_s^2$$

where, by (1.3.3),

$$V_s = V_{s_o} V^{\frac{1}{2}} \left\{1 + \frac{32}{5}\ \frac{A_p^2 V^6}{U^3 (1 + 8\ \frac{V^3}{U})}\right\}^{\frac{1}{2}} = V_{s_o} g_1(U,V,A_p),$$

where A_p is defined as the ratio of gas to radiation pressure at z = o.

$$\therefore\ P + P_t = \frac{k}{M_p}\ \rho_o T_o \{UV + A_p V^4 + \alpha^2 A_s g_1^2\} = \frac{k}{M_p}\ \rho_o T_o f_1(U,V,\alpha,A_p,A_s)$$

with $A_s \equiv \dfrac{V_{s_o}^2}{\frac{kT_o}{M_p}}$. Substitution into (2.1.6) then gives

$$\frac{df_1}{dy} = -2yU(1 + \alpha_o^2)A_s \qquad (2.1.19)$$

Furthermore,

$$C_p = \frac{C_{p_o}}{\gamma}\ \left\{1 \mp \frac{(4-3\beta)^2(\gamma-1)}{12\beta(1-\beta)(\gamma-1)\ +\beta^2}\right\}\ \left\{\frac{12(1-\beta)(\gamma-1)\ +\ \beta}{\beta}\right\}$$

$$= \frac{C_{p_o}}{\gamma\beta^2}\ \{(4-3\beta)^2(\gamma-1)\ +\beta^2+12\beta(\gamma-1)(1-\beta)\} = C_{p_o} g_2(\gamma,\beta)$$

(2.1.20)

where

$$\beta \approx \frac{P_g(1+\alpha^2)}{P_r+P_g(1+\alpha^2)} = \frac{1+\alpha^2}{1+\alpha^2+A_p V^3/U} \quad (P_g > P_r)$$

$$\beta \approx \frac{P_g}{(1+\alpha^2)P_r+P_g} = \frac{1}{1+(1+\alpha^2)A_p V/U} \quad (P_r > P_g)$$

in (2.1.20) only. (2.1.14) can now be written

$$(\alpha_o \rho_o V_{s_o} C_{p_o} T_o)\alpha' U g_1 g_2 \beta(y) \frac{dv}{dy} + \frac{4}{3} \frac{acT_o^4}{Z_o \rho_o K_e} \frac{V}{U\left(\frac{K}{K_e}\right)} \frac{dv}{dy} = \frac{2}{x_2} Q \int_o^y \beta(y)\alpha' U V^{\frac{1}{2}} dy$$

or

$$\alpha' U g_1 g_2 \frac{dv}{dy} + A_f \frac{V^3}{\left(\frac{K}{K_e}\right)_U} \frac{dv}{dy} = \left[\frac{2Q}{\alpha_o \rho_o V_{s_o} C_{p_o} T_o X_2}\right] \int_o^y \beta\alpha' U V^{\frac{1}{2}} dy \qquad (2.1.21)$$

where $A_f \equiv \dfrac{4acT_o^3}{3\alpha_o \rho_o^2 V_{s_o} Z_o C_{p_o} K_e}$.

Boundary conditions for (2.1.19), (2.1.21) are obviously $U = V = 1$ at $y = o$.

The criterion (1.3.14) for stability against convection can also be put in dimensionless form:

$$\left(1 - \frac{1}{\Gamma^2}\right) \frac{T}{P} \frac{\partial P}{\partial Z} < \frac{\partial T}{\partial Z}$$

$$\therefore \quad \left(1 - \frac{1}{\Gamma^2}\right) \frac{V}{f_1} \frac{df}{dy} < \frac{dv}{dy}$$

which becomes

$$-\frac{dv}{dy} < 2\left(1 - \frac{1}{\Gamma^2}\right) \frac{V}{f_1} YU(1+\alpha_o^2)A_s \qquad (2.1.22)$$

where the last approximation is valid if $Y_1\sqrt{\frac{2T_o}{T}} \gg 1$ (e.g. optically thick disks). If electron scattering is dominant for $Z \gtrsim Z_1$, the effective optical depth can be shown to be

$$\tau_{Z_1} = \tau_{Z_1}(\bar{\kappa})\,\tau_{Z_1}(K_c) \approx \frac{1}{2} K_e Z_o \frac{\rho_o}{Y_1} \frac{U_1^3 V_1^{-3/2}}{A_a} , \qquad (2.1.25)$$

$$A_a \equiv \frac{K_e}{b\rho_o T_o^{-7/2}} .$$

Clearly, the vertical optical depth of an arbitrary point in the disk is then given by $\tau_Z = \tau_{Z_1} + \tau_o - \tau_{oZ}$, where $\tau_o \equiv$ total optical thickness of the disk, $\tau_{oZ} \equiv$ optical thickness of layer (o,Z).

IV. An application : absorption line profiles

In view of the poorly determined and also controversial estimates of the disk mass, comparison of theoretical and observed line spectra seems to offer the only way of discriminating between the consequences of different viscosity laws by empirical means. It should therefore be attempted to use theory for the profiles which is at least order of magnitude correct. Unfortunately existing material is of little use here; all authors seem to have disregarded z-variation of physical quantities in disks. Papers addressing specifically disks in CVs (Smak 1969, Gorbatsky 1965) furthermore assumed optically thin disks. A more detailed treatment will be attempted here.

Formulation of the problem

Let the angle between the line of sight and the perpendicular to the disk (z-axis) be i. The x and y axes lie in the plane of the disk; the x-axis is chosen in the plane defined by the z-axis and line of sight. (The angle between x-axis and line of sight is then $i' = \pi/2 - i$).

For the intensity of radiation emitted by a unit surface area on the disk we have

$$I_\lambda(\theta) = \int_0^{+\infty} S_\lambda(\tau_\lambda, \theta) e^{-\tau_\lambda \sec\theta} \sec\theta \, d\tau_\lambda \qquad (3.1.1)$$

where θ is the angle between the line of sight and the normal to the unit area, S_λ is the source function and τ_λ is the optical depth of the atmosphere to radiation of wavelength λ

($\tau_\lambda \equiv o$ at the top of the atmosphere).

The following approximations are made: (a) The disk is flat (i.e. thickness independent of z so that surface normals are parallel to the z-axis). (b) LTE holds throughout the atmosphere.

The total monochromatic flux, neglecting all contributors but the disk, as well as obscuration by the central star, is then given by

$$F_\lambda(i) = \sec i \, d\Omega \int_{R_s}^{R_d} RdR \int_o^{2\pi} d\psi \int_o^{\infty} B_{\lambda'}(\tau_{\lambda'}) e^{-\tau_\lambda \sec i} \, d\tau_{\lambda'}, \tag{3.1.2}$$

Here $d\Omega$ is the solid angle subtended by the observer and λ' is the wavelength of radiation emitted by the disk such that the observer sees it as at wavelength λ , i.e.

$$\lambda' = \lambda\left(1 - \frac{V_*}{c}\right) = \lambda\left(1 - \frac{V_\theta \sin\psi \cos i'}{c}\right) \tag{3.1.3}$$

if V_θ is assumed independent of Z. V_* is the projection of the Keplerian velocity on the line of sight, positive for points receding from the observer.

B_λ, in (3.1.2) is the Planck function,

$$B_\lambda \equiv \frac{2hc^2}{\lambda^5} \left[\exp\left(\frac{hc}{\lambda kT}\right) - 1\right]^{-1} \tag{3.1.4}$$

We also have

$$d\tau_{\lambda'} \equiv (K_{\lambda'} + \ell_{\lambda'} + \sigma_{\lambda'})\rho dx \tag{3.1.5}$$

$$\tau_{\lambda'} \equiv \int_o^x d\tau_{\lambda'}, \tag{3.1.6}$$

where: $x \equiv$ geometrical depth in the atmosphere, measured positive downward and with origin at the surface ($\tau = o$)

$K_\lambda, \equiv$ monochromatic absorption coefficient

$\ell_\lambda, \equiv$ line absorption coefficient

$\sigma_\lambda, \equiv$ scattering coefficient

If the variation of temperature and density with x is assumed to be known, it remains only to specify the dependence of the coefficients above on ρ, T, λ'. In the next two subsections the absorption coefficients are written in terms of λ' , T and various number densities.

Monochromatic absorption coefficient

If we restrict ourselves to the lower members of the hydrogen Balmer series, for which results have been published, absorption by elements heavier than helium can probably be disregarded in the calculation of τ_λ - these elements absorb mainly on the blue side of the Balmer limit (e.g. Swihart 1956). Molecular absorption will be neglected as the disk is expected to be appreciably ionized. Free-free absorption by H^- is neglected. compared to the bound-free process as the former is dominant only for $\lambda \gtrsim 13{,}000$ Å (Aller p.192). Since Thomson scattering is included, Rayleigh scattering will be neglected (CG p.393).

The remaining sources of continuum opacity are:

(a) HI

The contribution of both bound-free and free-free processes can be approximated by

$$\rho K_\lambda(HI) \approx \frac{2N(HI)}{U(HI,T)} \quad \frac{K}{c^3} \; e^{-\alpha_1} \left\{ \sum_{n=n^*}^{8} \frac{e^{\alpha_n}}{n^3} + \frac{e^{\alpha_8}}{2\alpha_1} \right\} \qquad 3.1.7)$$

(Münch p.30, Mihalas p.119). Symbol meanings are:

$N(HI)$ ≡ number of HI atoms per cm^3

$U(HI,T)$ ≡ partition function of HI

K ≡ constant = 2.815×10^{29}

$\alpha_n \equiv \frac{h\nu_n}{kT} = \frac{R}{n\ kT}$, R being the Rydberg constant

For given λ , n^* is the smallest integer satisfying $n^* \geq \left(\frac{R\lambda}{hc}\right)^{\frac{1}{2}}$

(b) He I (b-f)

Since the absorption edges of quantum states for which accurate cross sections are available all lie beyond the Balmer limit (Mihalas p.121), we will use the simple hydrogenic approximation (Münch p.32):

$$\rho K_\lambda(HeI,b\text{-}f) \approx \frac{K\lambda^3 e^{-\alpha_1}}{c^3 U(HeI,T)}\ N(HeI) \left\{ \sum_{n^*}^{8} \frac{e^{\alpha_n}}{n^3} + \frac{e^{\alpha_8} - 1}{2\alpha_1} \right\} \qquad (3.1.8)$$

(c) He I (f-f)

Mihalas (p.122) gives

$$\rho K_\lambda(HeI,f\text{-}f) = N(HeI)\ \frac{U(HeII,T)}{U(HeI,T)}\ \frac{K\lambda^3}{c^3}\ \frac{\exp - \left\{\frac{\chi_I(HeI)}{kT}\right\}}{\chi_I(HI)/kT} \qquad (3.1.9)$$

where $\chi_I(HeI)$, $\chi_I(HI)$ are the ionization potentials of neutral helium and hydrogen respectively.

(d) He II

According to Mihalas

$$\rho K_\lambda(\text{HeII}) \approx \frac{32N(\text{HeII})}{U(\text{HeII},T)} \frac{K\lambda^3}{e^3} e^{-\alpha_1} \left\{ \sum_{n^*}^{8} \frac{e^{\alpha_n}}{n} + \frac{e^{\alpha_8}}{2\alpha_1} \right\} \qquad (3.1.10)$$

where now $\alpha_n = \frac{4R}{n^2 kT}$, n^* is the smallest integer satisfying $n^* \geq 2\left(\frac{R\lambda}{hc}\right)^{\frac{1}{2}}$.

(e) $\underline{H^-}$

The polynomial

$$a_\lambda(H^-) = -0.37 + 0.5564\,\lambda + 5.2375 \times 10^{-2}\,\lambda^2 - 7.9167 \times 10^{-3}\,\lambda^3 + 1.25 \times 10^{-4}\,\lambda^4$$

(λ in units of 10^3 Å) provides a good fit to the bound-free coefficient of Doughty & Fraser (1966) over the Balmer region. The absorption coefficient is

$$\rho K_\lambda(H^-) = N(H^-)\,a_\lambda(H^-) \qquad (3.1.11)$$

(f) Thomson scattering

The scattering cross section of a free electron is 6.654×10^{-25} cm^2, so that

$$\rho\sigma_o = 6.654 \times 10^{-25}\, N_e \qquad (3.1.12)$$

independent of λ.

Line absorption coefficients : broadening mechanisms

(a) Doppler broadening

The absorption is given by

$$\rho\ell_\lambda(\text{Doppler}) = \frac{\sqrt{\pi}\, e^2}{M_e c} \frac{\lambda_o^2 \tilde{N}}{\Delta\lambda_D} \exp - \left(\frac{\Delta\lambda}{\Delta\lambda_D}\right)^2 \qquad (3.1.13)$$

where λ_o is the central wavelength of the line, $\Delta\lambda = \lambda - \lambda_o$, $\tilde{N}$ is the number density of the absorbing atoms (i.e. number density of hydrogen atoms in quantum state n = 2), and

$$\Delta\lambda_D \equiv \frac{\lambda_o}{c} \sqrt{V_s^2 + V_t^2} \qquad (3.1.14)$$

(b) Stark broadening

For the linear Stark effect we adopt an expression due to Griem, Kolb & Shen (1959):

$$\rho\ell_\lambda(\text{Stark}) = \frac{\tilde{N} C_n E_o^{3/2}}{(\Delta\lambda)^{5/2}} \left\{1 + R(N_e,T) \sqrt{\Delta\lambda}\right\} \qquad (3.1.15)$$

where C_n are tabulated constants (e.g. Aller p.332), $E_o \equiv 2.6 \times e N_i^{2/3}$, e electronic charge, $N_i \equiv$ number of singly ionized perturbing ions/unit volume, and $R(N_e,T)$ are constants tabulated by Griem et al. This formula is valid in the line wings and takes into account both quasi-static broadening by ions and impact broadening by electrons. Although it overestimates absorption at very large displacements from the line centre (e.g. Mihalas p.293), it should be adequate for our purpose (Aller p.332). (Furthermore, only interaction with singly ionized atoms is taken into account. Since hydrogen is itself appreciably ionized under conditions where the number density of multiply-ionized atoms is large, this should, however, not be serious.)

We shall not include the quadratic Stark effect, resonance broadening or radiation damping here; only a crude validity criterion for neglecting these effects will be obtained. For resonance broadening (cubic Stark effect) Mihalas (p.296) quotes the damping constant $\Gamma_c = \frac{4}{3} \frac{N_o e^2}{M_e} \lambda_o f_{ij}$. ($N_o \equiv$ number of neutral atoms of the line-producing species/unit volume, $f_{ij} \equiv$ oscillator strength for the relevant transition.) Resonance broadening will dominate over natural broadening provided $\Gamma_c \gg \Gamma_r$, Γ_r being the radiation damping constant for the line. Using the classical expression for Γ_r and setting $f_{ij} \sim 1$, we find that resonance broadening dominates provided $N_o \gg \frac{2\pi^2}{\lambda_o^3}$. Compared to the linear Stark effect it (resonance broadening) is important if $\frac{N_o}{N_e} \gtrsim 10^4$ (Aller p.333). Thus provided $N_e \gtrsim 10^{-4} N_o$, $N_o \gg \frac{2\pi^2}{\lambda^3}$ both natural and resonance broadening can be neglected.

For the ratio of linear to quadratic Stark absorption, Edmonds et al. (1967) quote a lower limit $\frac{10^{16}}{n^4 N_e^{2/3}}$, n being the principal number of the upper state. If $n \lesssim 6$, the quadratic effect can be neglected for $N_e \lesssim 10^{19}$ cm^{-3}.

The total absorption coefficient, corrected for induced emission, is given by

$$\rho(K_\lambda + \ell_\lambda + \sigma_\lambda) = \{\rho K_\lambda(\text{HI+HeI+HeII+H}^-) + \rho\ell_\lambda\ (\text{Doppler}) + H(|\lambda - \lambda_1|)\rho\ell_\lambda(\text{Stark})\} \times \left[1 - \exp\left(\frac{hc}{\lambda kT}\right)\right] + \sigma\rho \qquad (3.1.16)$$

where H is a step function which is zero in the Doppler core of the line.

The calculation of the various number densities and P_e for given ρ, T is to be performed in the standard way.

V. Computational Details

Disk models

The equations governing the disk structure were solved for a $1M_\odot$, $R_s = 10^9$ cm central star, using the SS viscosity law with $\alpha \equiv$ constant, i.e. independent of position. To illustrate the influence of turbulent velocity and mass transfer rate on the disk structure, three models were constructed:

(1) $\alpha = 1$, $\dot{M} = 10^{17}$ g/sec

(2) $\alpha = 1$, $\dot{M} = 10^{18}$ g/sec

(3) $\alpha = 10^{-2}$, $\dot{M} = 10^{17}$ g/sec.

At each radial position the following procedure was adopted: a starting value for T_o was found by guessing the ratio $\frac{q_z^{(t)}}{q_z^{(r)}}$ $(z = o)$ and solving for T_o. (Since this ratio varies slowly over the greater part of the disk, the method provided good first estimates.) Z_o, U_o and ρ_o could then be found from (2.1.1), (2.1.12) and (2.1.10). Integration of (2.1.19) and (2.1.21) was performed by the standard Runge-Kutta method. Outward (i.e. towards larger z) rather than the usual inward integration was used because both boundary values and the position of the boundary ($\tau = o$) at the top of the atmosphere were unknown. No problems with numerical instabilities were encountered: for small α and R, however, convergence was slow.

The opacity at each integration step was found by inter-

polation in the X = 0.8, Z = 0.01 - tables of Cox & Stewart (1970). Turbulent mixing lengths were determined iteratively. On completion of an integration cycle, the temperature at $\tau \sim 0.67$ was compared to the effective temperature (approximated by $T_{ef} \approx \left(\frac{Q}{\sigma}\right)^{\frac{1}{4}}$). The process was then repeated with a new value of T_o until satisfactory agreement was achieved. Whenever convective instablilty occurred, the temperature gradient was equated to the adiabatic gradient.

Since little stood to be gained by an exact determination of the X_i-factors, these were approximated. As V varies slowly over the region $|Z| < \beta_1 Z_o$; $X_1 \approx \int_{-\beta_1}^{\beta_1} U^2 \, dy = 2 \int_o^{\beta_1} U^2 \, dy$,

$X_2 \approx 2 \int_o^1 U \, dy \approx X_3$; and $q_z^{(t)} + q_z^{(r)} \approx \frac{2}{X_2} \, Q \int_o^Y \beta U dy$.

Furthermore, as radiation pressure should be unimportant in CV-disks, the behaviour of U is approximately Gaussian (see beginning of § III) and $X_2 \approx X_3 \approx \sqrt{\pi}\ \mathrm{erf}(1) \approx 3/2$.

The factor A_s in (2.1.19) was taken as unity.

Line profiles

The profile of the H_β-line was computed for the three models of the previous section. The three dimensional integration was performed in the order given in (3.1.2) for a number of values of i and R_d . Only one half of the observable profile was calculated, symmetry being assumed.

(i) τ-integration

(This gives the intrinsic profile I_λ of an infinitesimal annulus.)

For a given radial position, the previously computed temperatures and densities were read in and used to compute the monochromatic and line absorption coefficients at a number of vertical positions. $X = 0.73$, $Y = 0.25$ were used. Elements heavier than He were represented by a "mean" metal for which the abundances and ionization potentials were adjusted to give agreement with tabulated opacities. Partition functions were taken to be constant.

It was found necessary to exclude He I(b-f) absorption, as the crude formula (3.1.8) led to severe overestimates. Calculated opacities finally agreed to within 25% with tables (Allen 1973 pp.100 f) for $0.1 \leq \theta \leq 0.8$. Large deviations from published values at $\theta = 1$ and high P_e are probably due to pressure ionization being ignored (see original source of tabulations, Bode 1965). Fortunately, these conditions did not occur in any of the models. The monochromatic absorption was evaluated at the central wavelength λ_o 4861 Å of the line only.

Two-way logarithmic interpolation in the tables of Griem et al. (1959) was used to find the electronic contribution to the Stark absorption. N_i was set equal to N_e. Near the line centre the Stark absorption was kept constant at its value at $\lambda_* = \lambda_o - 0.05\, E_o \approx \lambda_o - 6.25 \times 10^{-11} N_e^{2/3}$ (see H_β-graph of Edmonds et al. 1967).

Once the absorption coefficients had been calculated, τ could be found from (3.1.5), (3.1.6) and (3.1.16). It was convenient to use the substitution $x = e^{-\tau_\lambda}$, so that

$$I_\lambda(i) = \int_o^{+\infty} B_\lambda(\tau_\lambda)\, e^{-\tau_\lambda \sec i}\, d\tau_\lambda = \int_o^1 B_\lambda(x) x^{\sec i - 1}\, dx.$$

The integral was evaluated numerically by assuming that B varies linearly over each step (rather than the usual assumption of constancy). Thus

$$I_\lambda \approx \sum_{i=o}^{+\infty} \frac{1}{2} [B(X_{i+1}) + B(X_i)] [\frac{1}{2} (X_{i+1} + X_i)]^{\sec i - 1} (X_{i+1} - X_i).$$

It was assumed that the intrinsic profile is symmetrical with respect to λ_o .

(ii) ψ-integration

(This gives the observed profile $\int I_\lambda$, of an infinitesimal annulus.)

Simpson's rule was used to integrate I_λ over the interval $-\pi/2 \leq \psi \leq \pi/2$. For specified ψ and λ , λ' was calculated from (3.1.3). I_λ, was then found by quadratic interpolation in I_λ .

(iii) R-integration

Step sizes were varied from 0.25 in the inner parts of the disk to 2 for large R, giving ~35 steps in all. Solution was obtained by trapezoidal-type integration.

VI. Results

Radial structure of the disk

The variation of T_o , ρ_o and Z_o with r for the three models under consideration is illustrated in figs. 1-3. Estimated disk masses, lifetimes and luminosities are given in table 1.

Table 1

		Model 1	Model 2	Model 3
	M_d(g)	4.4×10^{22}	1.5×10^{23}	2.4×10^{24}
	τ_ℓ(sec)	4.4×10^{5}	1.5×10^{5}	2.4×10^{7}
	L_d(erg sec^{-1})	6×10^{33}	6.1×10^{34}	6.1×10^{33}
L_{st}	$\varepsilon = o$	7×10^{33}	7×10^{34}	7×10^{33}
(erg/sec)	$\varepsilon = 1$	4×10^{32}	3.6×10^{33}	3.6×10^{32}

(Provided the sense of rotation of the white dwarf is the same as that of the orbital motion in the disk, $o \leq \varepsilon = \frac{\omega_s}{\sqrt{\frac{GM}{R_s}}} \leq 1$, with $\varepsilon = o$ for a nonrotating star, $\varepsilon = 1$ for a star rotating at the limit of stability). Small differences in the luminosity-entries for models 1 and 3 are due to the fact that $R_d \approx 27\ R_s$ for the former, $R_d \approx 30\ R_s$ for models 2 and 3.

The values derived for M_d differ by several orders of magnitude from those of Smak (1972) and Warner (1974). In the introduction some objections against Smak's deduction were

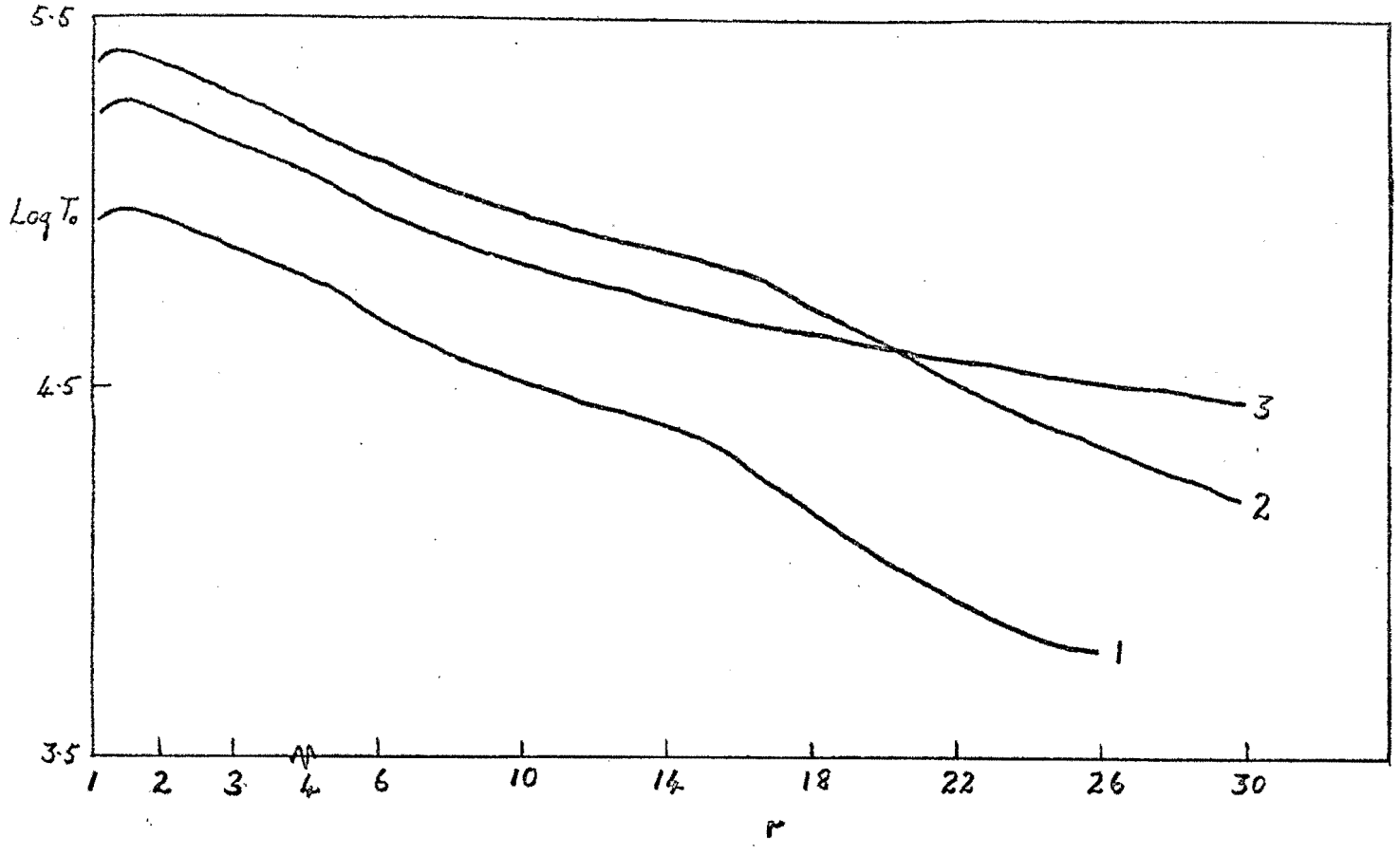

Figure 1. Temperature at Z = o as a function of radial distance for the three models

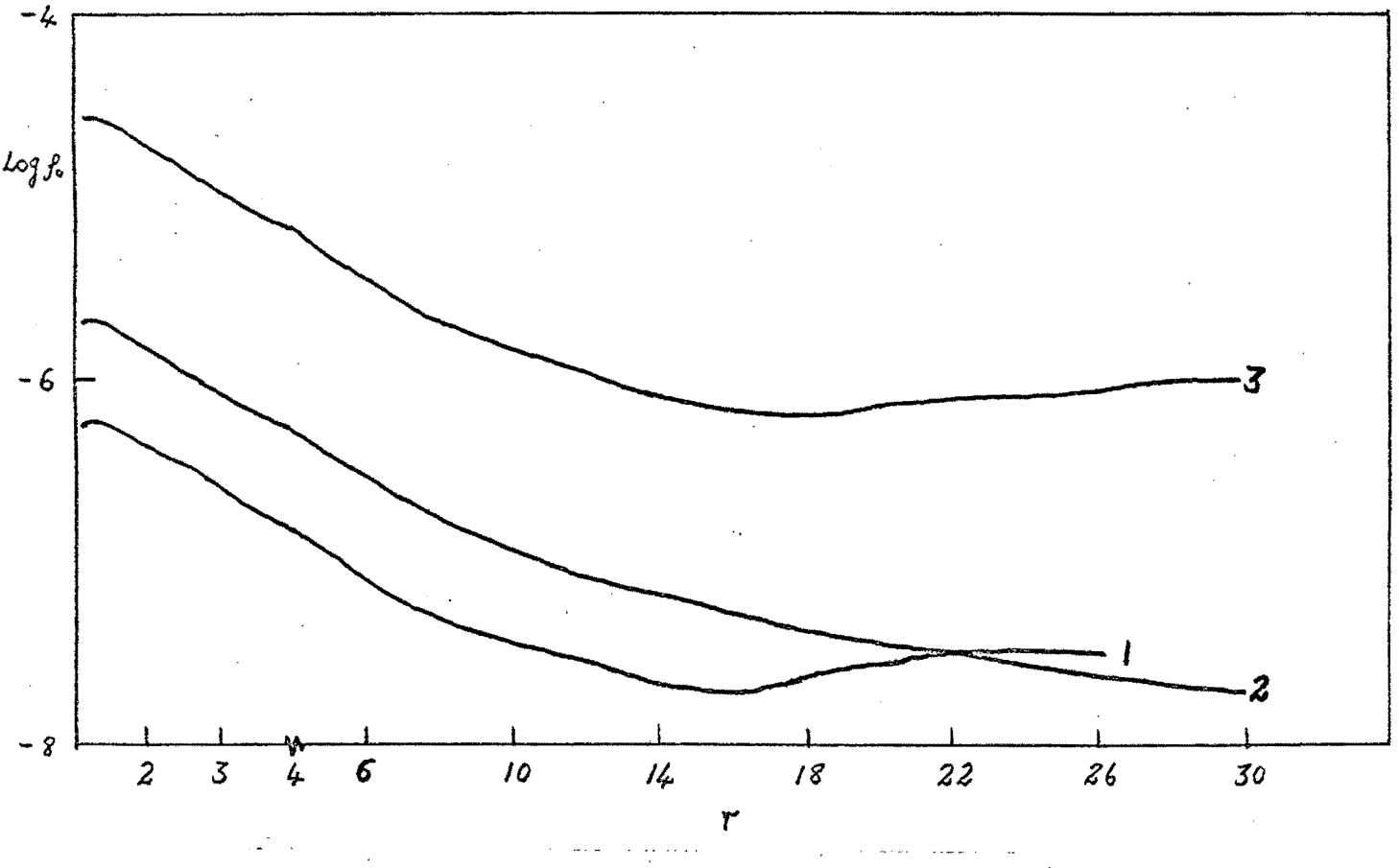

Figure 2. Density at Z = o as a function of radial distance for the three models

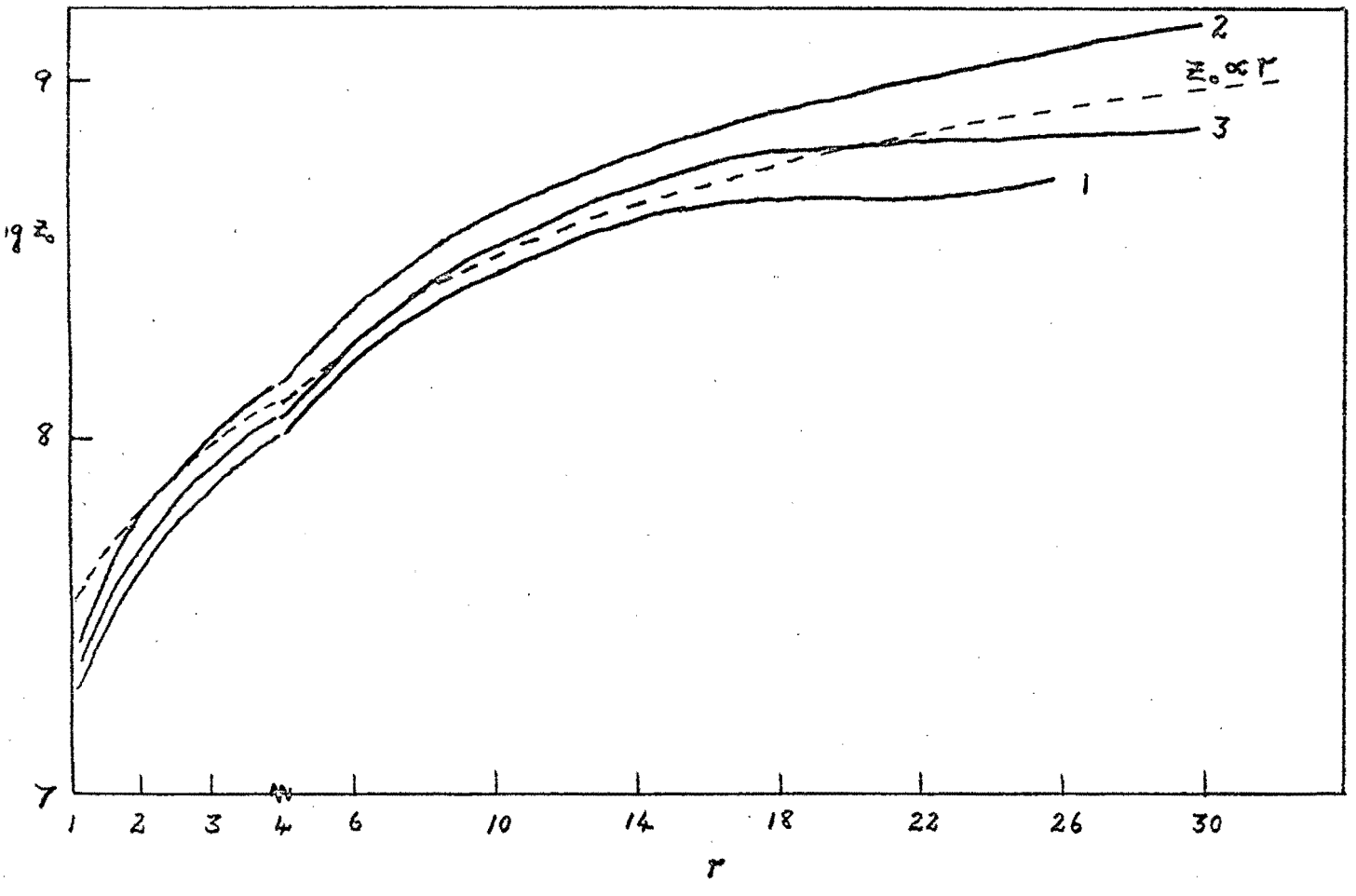

Figure 3. Vertical height scale as a function of radial distance for the three models

given, whereas Warner's parameters are not compatible with our models. The latter author used the rate of decline of the lightoutput of dwarf novae after outburst to derive $\overline{K}\ \overline{Z}_o\ M_d \sim 10^{37}$. Only the radiation energy density in the disk was included, while we find the thermal energy content is several orders of magnitude larger. (Ratio of radiation to thermal energy density $\approx$ ratio of radiation to gas pressure $\sim 10^{-3}$; see below.) Furthermore, the presence of convection zones in the disk (see subsection after next) implies a higher opacity than Warner's value $\overline{K} = K_e$. Inspection of figs. 1, 2 and Cox & Stewart's opacity table shows that $\overline{K}$ is generally 10-10^4 times larger than the electron scattering value $K_e \sim 0.3$. On the other hand, $\overline{Z}_o$ is smaller, say $\overline{Z}_o \sim 4 \times 10^8$ cm. Taking these effects into account, $\left(\frac{\overline{P}_g}{P_r}\right) \overline{Z}_o\ \overline{K}\ M_d \sim 10^{37}$ or $10^{22} \lesssim M_d \lesssim 10^{25}$ g is obtained so that our results are consistent with Warner's general theory.

Concerning the assumptions made in deriving the model equations we note that:

1) In all cases the ratio $\frac{|V_r|}{V_\theta}$ reaches a global maximum at the inner boundary r = 1.25 of the disk; values are 2×10^{-3}, 4×10^{-3} and 4×10^{-5} for models 1, 2 and 3 respectively.

2) The thin-disk approximation is valid as $\frac{2Z_o}{R}$ has maximal values 0.06, 0.09 and 0.07 in the three models. This also establishes the validity of assumption (ii) because

$$(1 + \alpha^2) \left(\frac{V_s}{V_\theta}\right)^2 = \frac{1}{2} \left(\frac{Z_o}{R}\right)^2 . \quad ((2.1.1), (2.1.2)).$$

3) Using lower limits to Z_o, ρ_o and upper limits to T_o from

the figures, we find $\frac{\alpha Z_o \rho_o}{T_o^2} > 5 \times 10^{-11}$, 2×10^{-11} , 2×10^{-12} for models 1, 2 and 3. This implies (equation (1.3.2)) that η_ℓ is negligible compared to η_t in all models.

Other interesting results are that radiation pressure is negligible in the core part of the disk (model 1: $3 \times 10^{-4} \lesssim \frac{P_r}{P_g} \lesssim 5 \times 10^{-2}$, model 2: $10^{-3} \lesssim \frac{P_r}{P_g} \lesssim 10^{-1}$ and model 3: $10^{-4} \lesssim \frac{P_r}{P_g} \lesssim 2 \times 10^{-2}$ at $Z = o$) and that turbulent conduction transfers a sizeable fraction of the total flux in this region. ($0.33 \lesssim \frac{q^{(t)}}{q^{(r)}} \lesssim 0.47$, $0.32 \lesssim \frac{q^{(t)}}{q^{(r)}} \lesssim 0.47$ and $0.86 \lesssim \frac{q^{(t)}}{q^{(r)}} \lesssim 0.94$ in the radiation zones of models 1, 2 and 3 respectively.) The total flux F was found slightly different from Q (see equation (2.1.14)) : $1.13 \lesssim F/Q \lesssim 1.28$. Also, the first scale height β_1 exceeded 1 by a few percent: $1.03 \lesssim \beta_1 \lesssim 1.11$.

The continuum spectrum

The continuum flux distribution $F_\lambda = 2\pi \int_{R_s}^{R_d} B_\lambda(T_{ef})\, RdR$ ($T_{ef} = \left(\frac{Q}{\sigma}\right)^{\frac{1}{4}}$, B_λ = Planck function) is shown in fig.4. For comparison two straight-line fits to the data of Szkody (1974) for SS Cyg are also drawn (arbitrary zero point). As mentioned in the previous subsection, the total flux might differ from Q; the resulting error in T_{ef} is, however, trivial (< 6½%) compared with other uncertainties.

In fig. 5 fluxes have been normalized to $F_{\lambda 1800} = 1$ for comparison with the observational results of Wu (1975). The only system which can be expected to conform to the steady-state

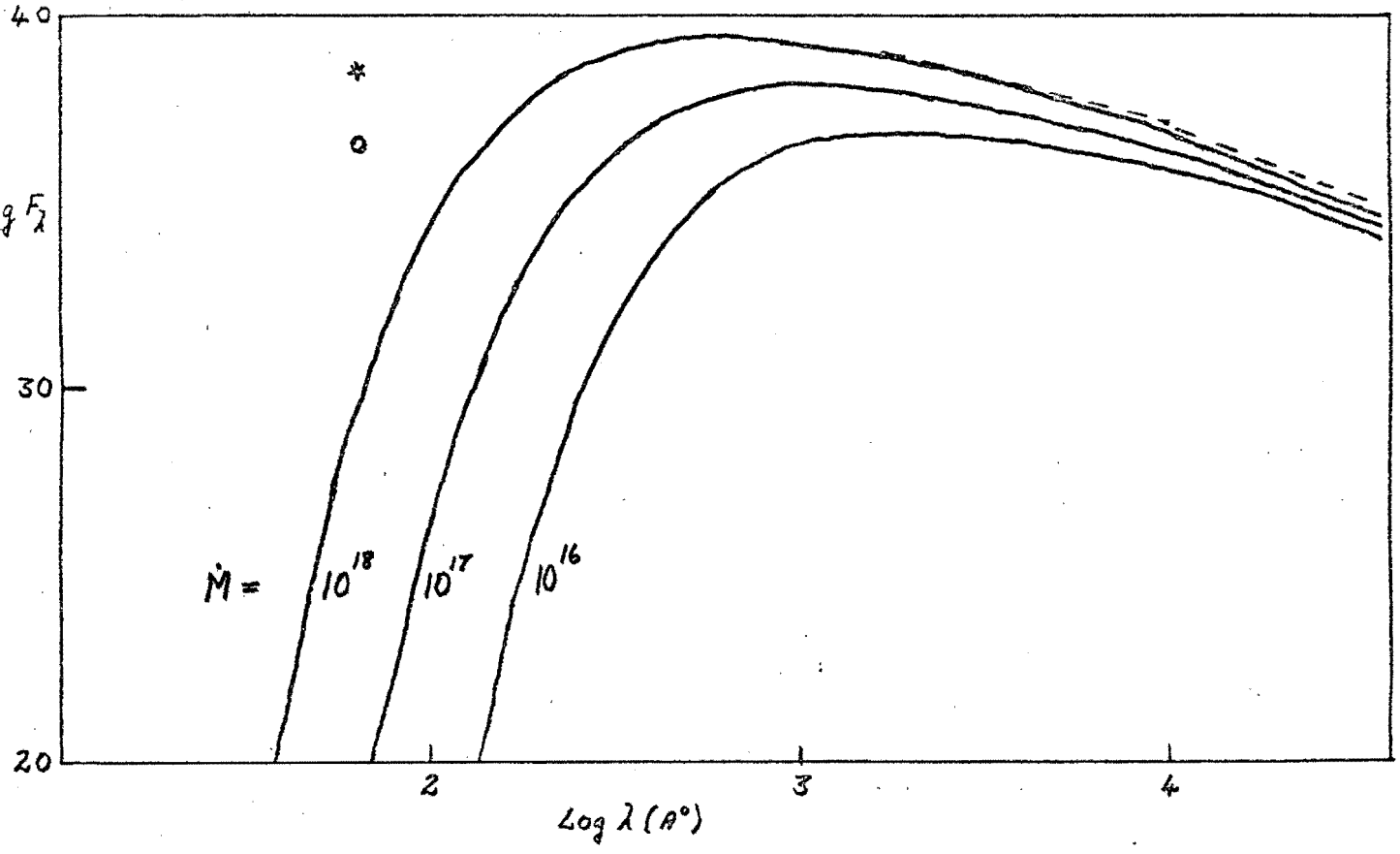

Figure 4. Continuum spectrum of the disk for a range of mass transfer rates. Observations of SS Cyg are indicated: (*) Rappaport et al. (o) Heise et al. (---) Szkody (see introduction).

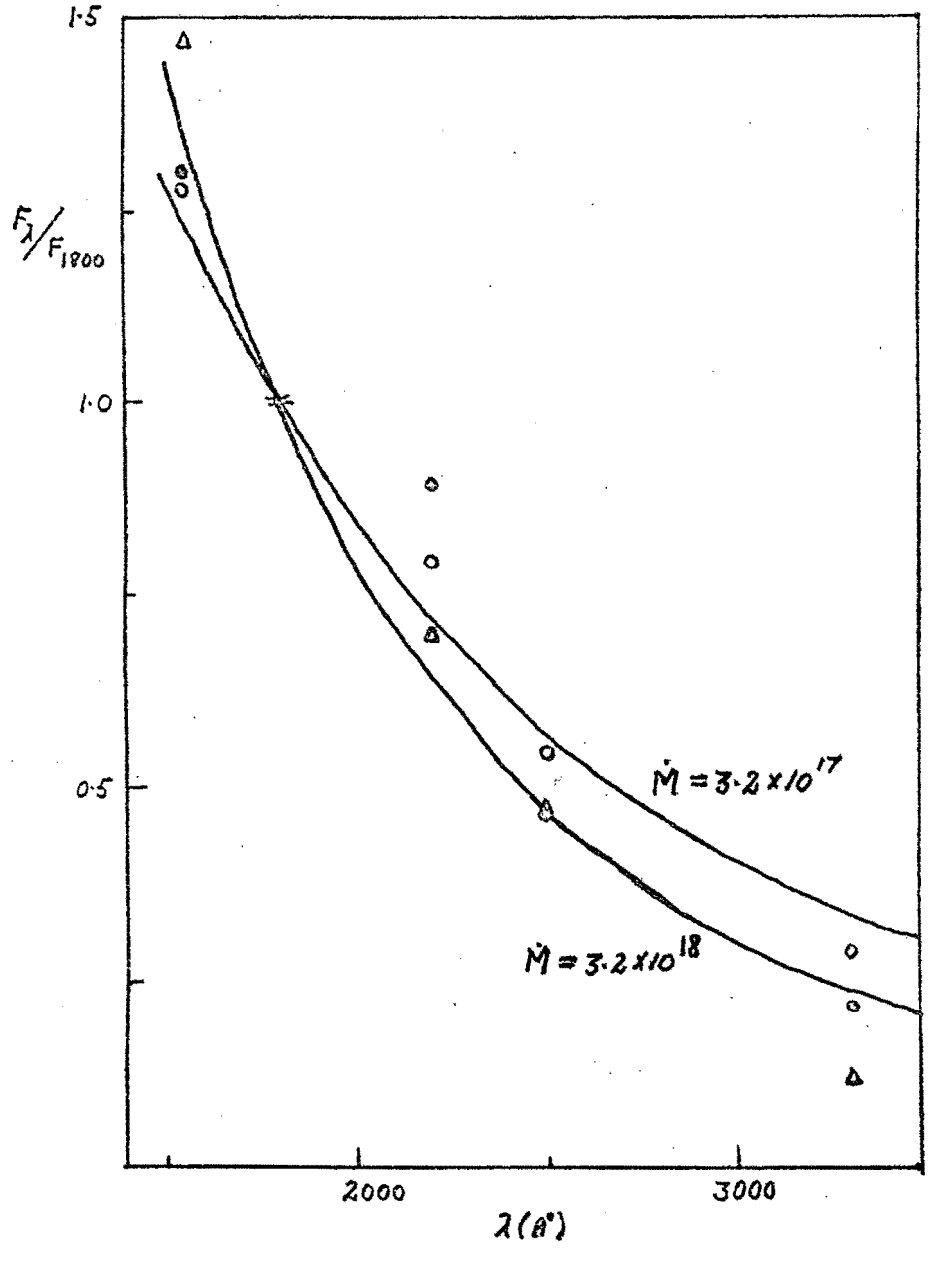

Figure 5. Comparison of model results with observations by Wu.
(o) Z Cam (standstill) (●) AR AND (maximum)
(Δ) U Gem (minimum)

assumption in an approximate manner in Z Cam, which was at standstill when observed. Agreement for the systems shown seems fair except at 2200 Å (Results for SS Cyg and SS Aur, however, differ appreciably from the calculated spectra.).

The effect of limb darkening was not included in our crude calculation and might alter the distributions.

The vertical structure of the disk

An example of the vertical structure of the atmosphere of the disk is shown in fig. 6 where the density and temperature variations for the three models are compared. All three atmospheres are radiative and have an effective temperature $\sim$ 11,500 ^{o}K; $4.67 \lesssim \log g \lesssim 4.82$, $4.20 \lesssim \log g \lesssim 4.33$ and $4.90 \lesssim \log g \lesssim 4.93$ in models 1, 2, 3 respectively. (The relatively small variation of log g in model 3 is due to the smaller geometrical extent of the region shown: 1) $1.31 \lesssim y \lesssim 1.85$ (2) $1.41 \lesssim y \lesssim 1.89$ (3) $1.83 \lesssim y \lesssim 1.98$). Note that, in contrast with stellar atmospheres, g increases towards smaller optical depths.

The extent of the convective regions in the disk is shown in figs. 7 and 8. (The surface $\tau = 0.01$ is also indicated. The geometrical shape of the disk can be found by modulating the results in fig. 3 with these curves.) It must again be pointed out that our treatment of convection is rather sketchy. In particular the approximation $\mu \equiv$ constant is incorrect and convection might also be superadiabatic. It was felt that in view of other uncertainties a more detailed treatment was not justified.

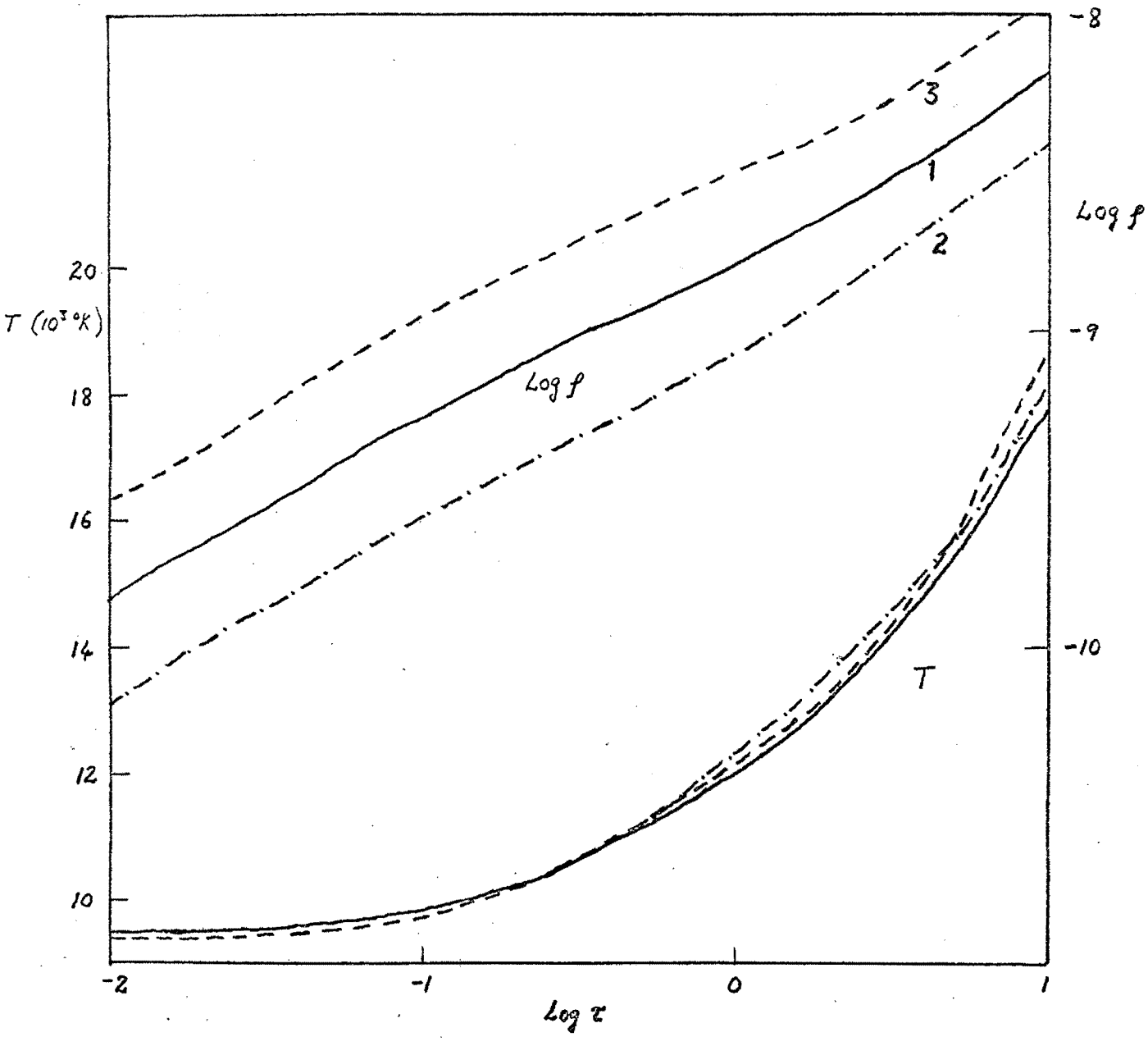

Figure 6. Vertical temperature and density profiles in the three models ($T_{eff} \sim 11{,}500\ ^{o}K$)

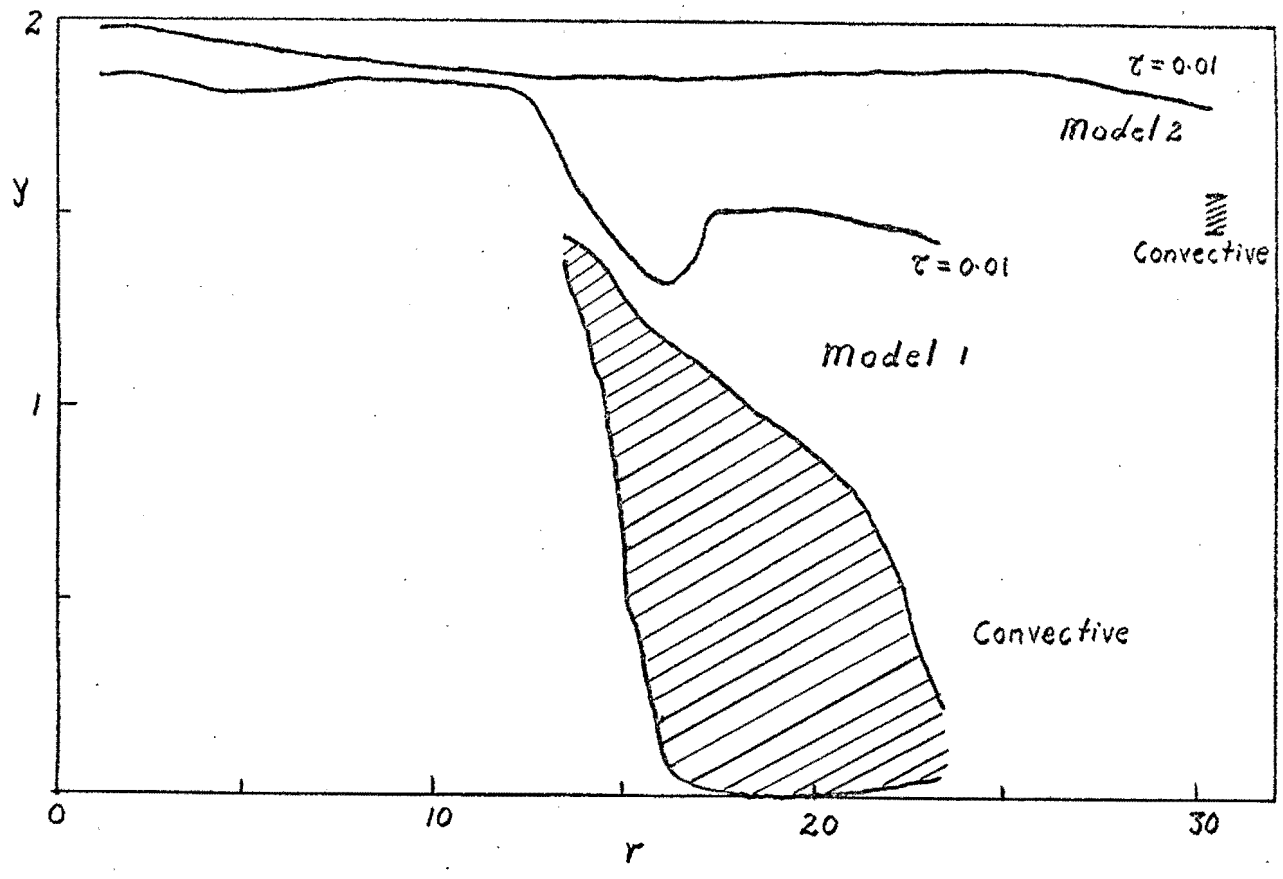

Figure 7. Convection zones in the disk (models 1 and 2)

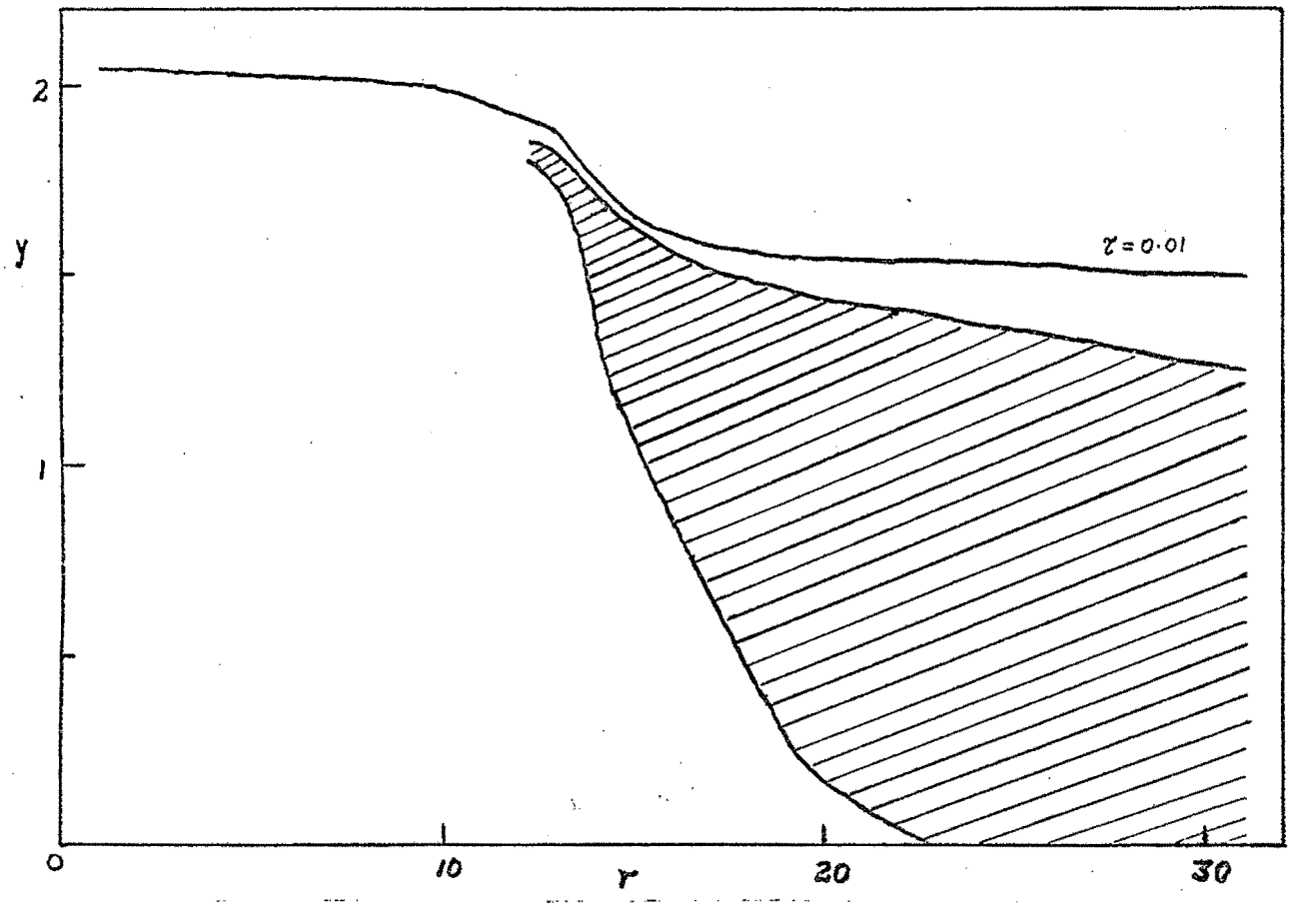

Figure 8. Convective zone in the disk (model 3)

In models 2 and 3, disks are optically thick for all R, $3 \times 10^2 \lesssim \tau_o \lesssim 6 \times 10^2$ for model 2 and $10^4 \lesssim \tau_o \lesssim 10^6$ for model 3. Model 1 was terminated at $R = 26\ R_s$ as the disk is optically thin at larger R. (This is also the reason for the shrinking of the convection zone of this model for $r > 21$.) For $1.25 \lesssim r \lesssim 19$ we have $2 \times 10^3 \lesssim \tau_o \lesssim 10^3$, decreasing to 130 at $r = 21$, 8 at $r = 23$.

Except for the region $15 \lesssim r \lesssim 21$ of model 2 where electron scattering is important above $\tau \sim 10^{-2}$, this absorption mechanism is negligible for $\tau > 10^{-3}$ in all our models.

Absorption line profiles

Results of the profile calculations are shown in figures 9-14. Inspection reveals the following characteristics:

(i) Profiles for model 3 are deeper than those for model 1. This is caused by the larger temperature gradients in the atmosphere of the model 3 disk. The continua are thus formed at higher, the line centres at lower temperatures than in model 1. Another source of small differences in line shapes is the absence of significant turbulent broadening in model 3 $\left(\frac{V_t}{V_s} = 10^{-2} \text{ as compared to } \frac{V_t}{V_s} = 1 \text{ in model 1.} \right)$

(ii) Line depths increase with increasing R_d. This is a consequence of adding low temperature regions in which hydrogen is less ionized than in the inner parts of the disk. In other words, the mean absorptional capability of the atoms is enhanced at greater R_d.

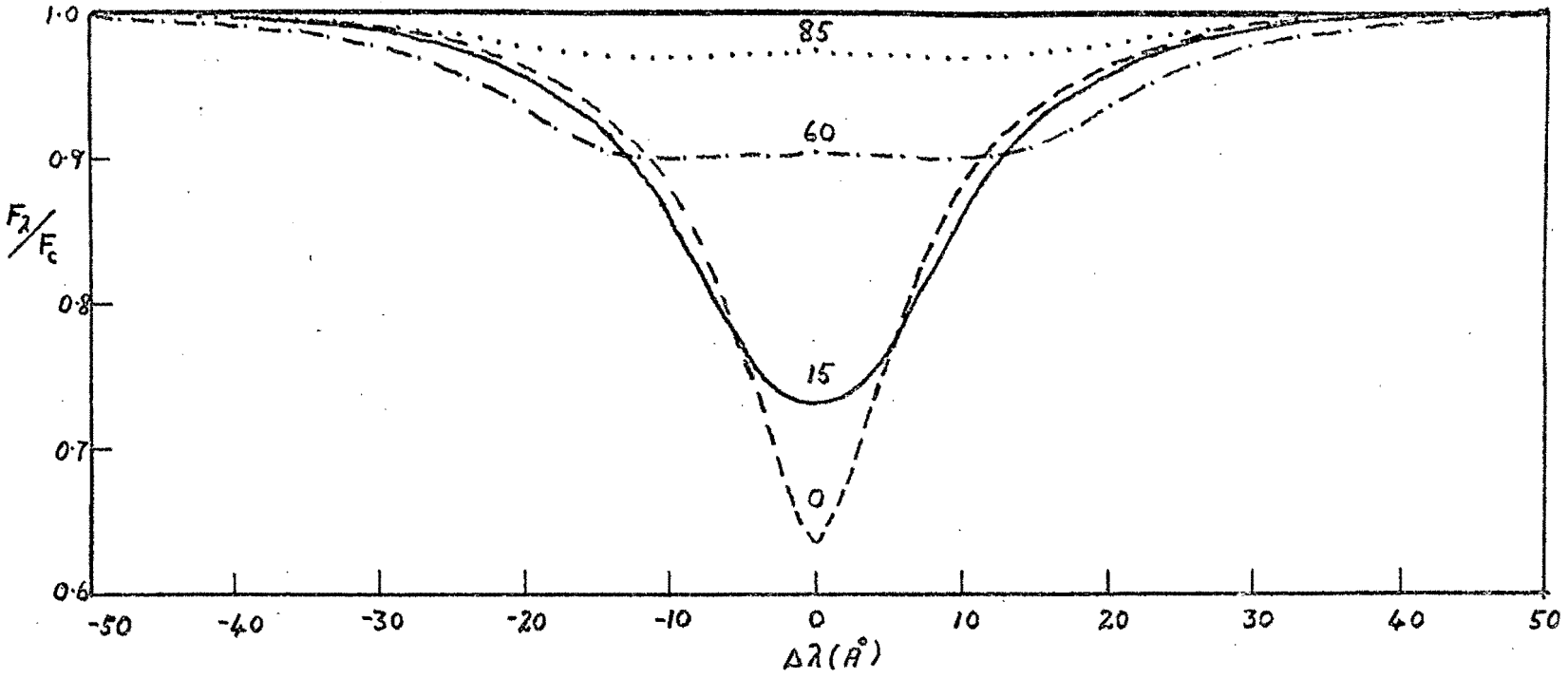

Figure 9. H_β absorption line profiles for model 1 with $R_d = 14\ R_s$. (Curves are labelled with values of i)

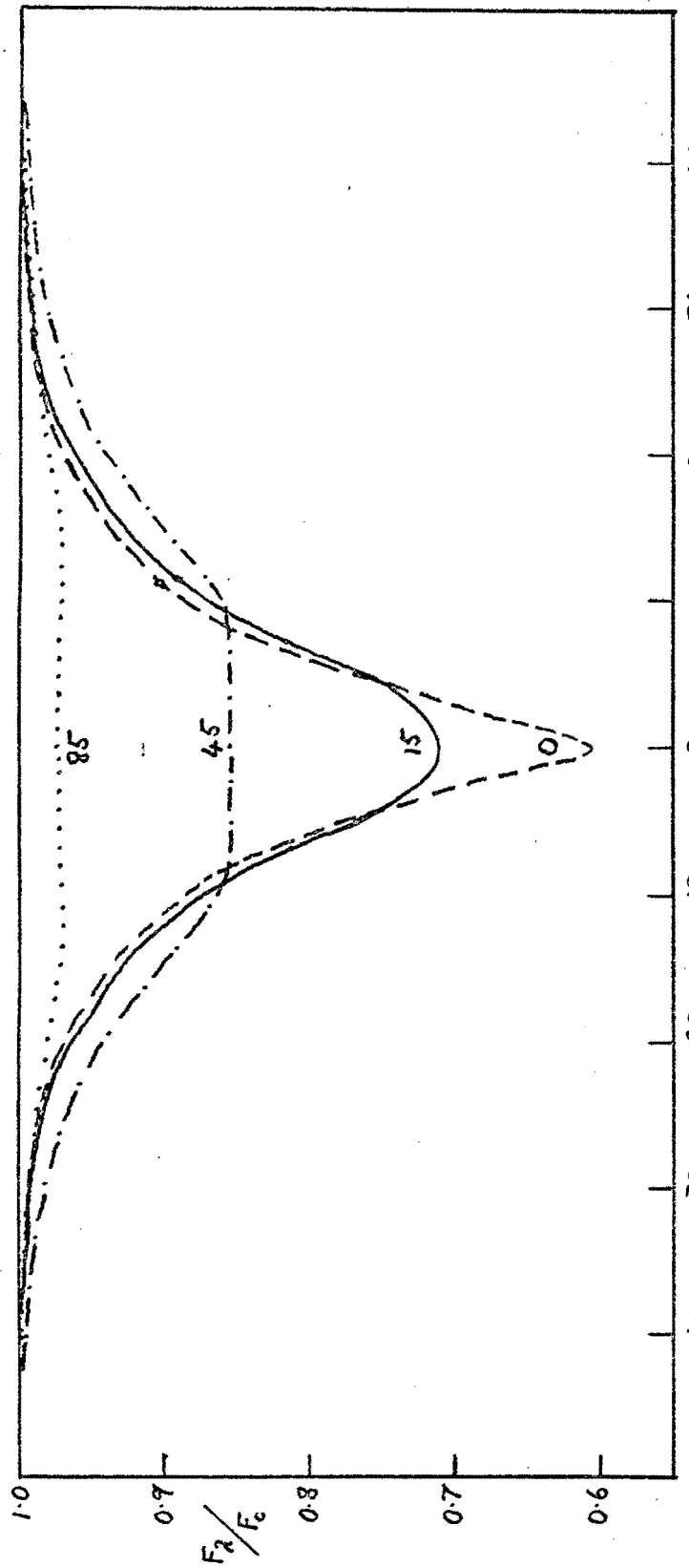

Figure 10. H_β absorption line profiles for model 1 with

$R_d = 21\ R_s$

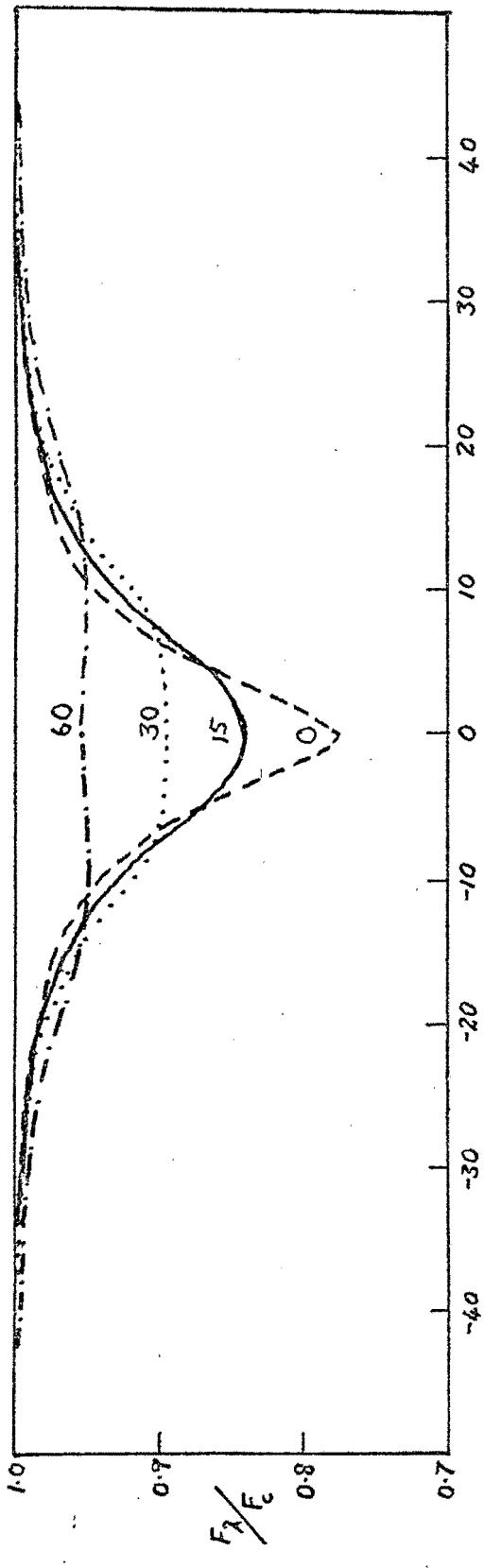

Figure 11. Hβ absorption line profiles for model 2 with

$R_d = 14\ R_s$

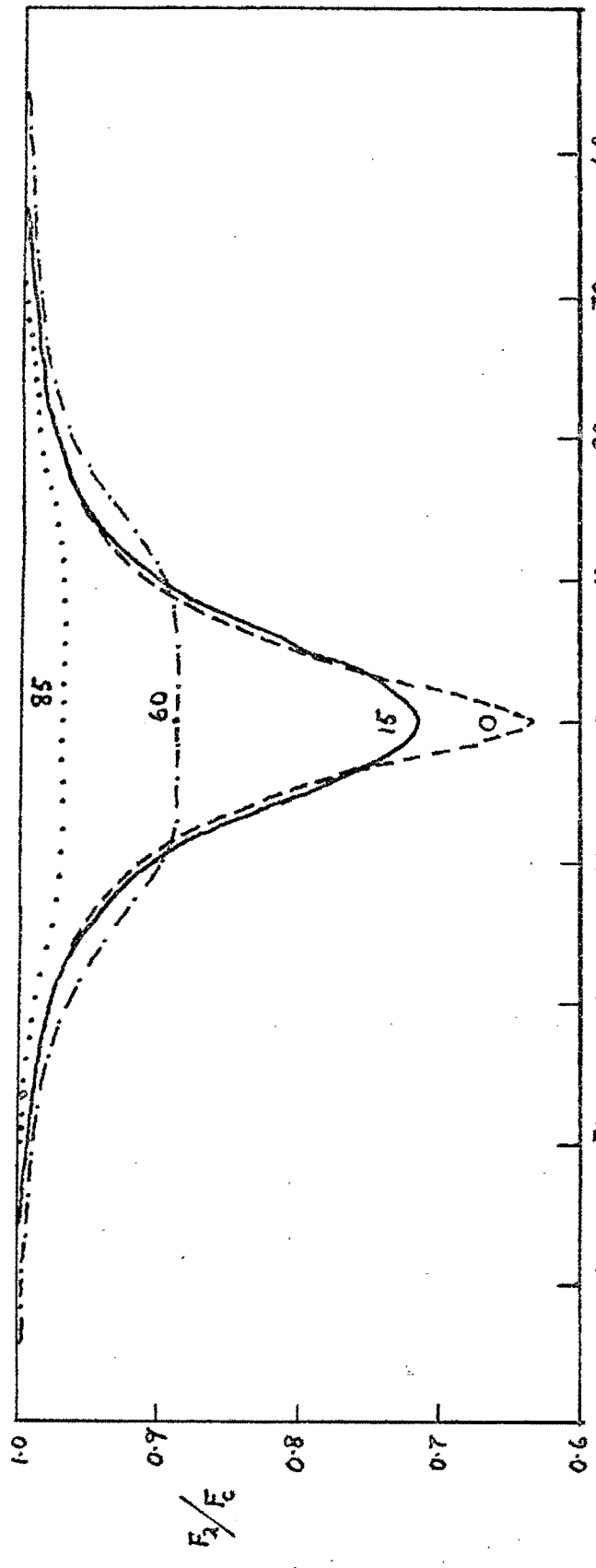

Figure 12. H_β absorption line profiles for model 2 with $R_d = 30\ R_s$

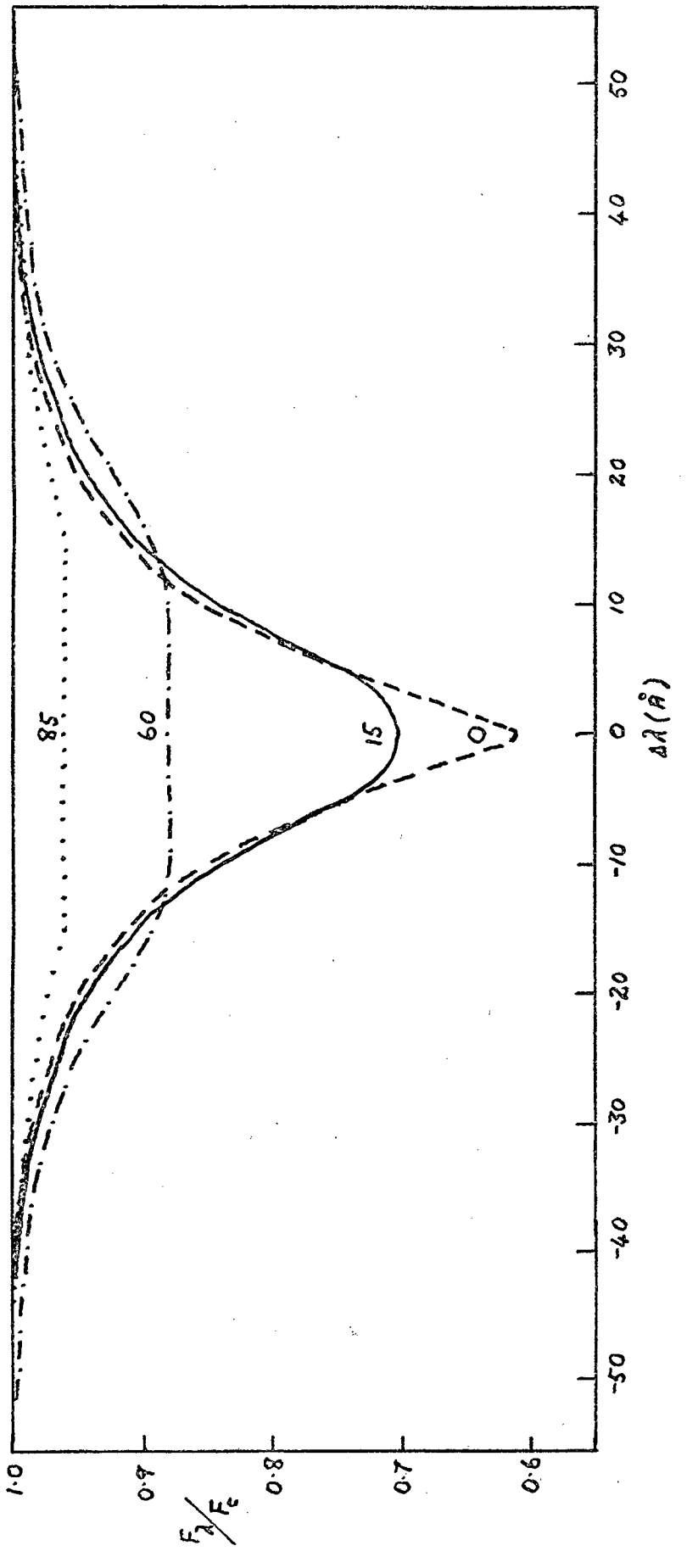

Figure 13. H_β absorption line profiles for model 3 with

R_d = 14 R_s

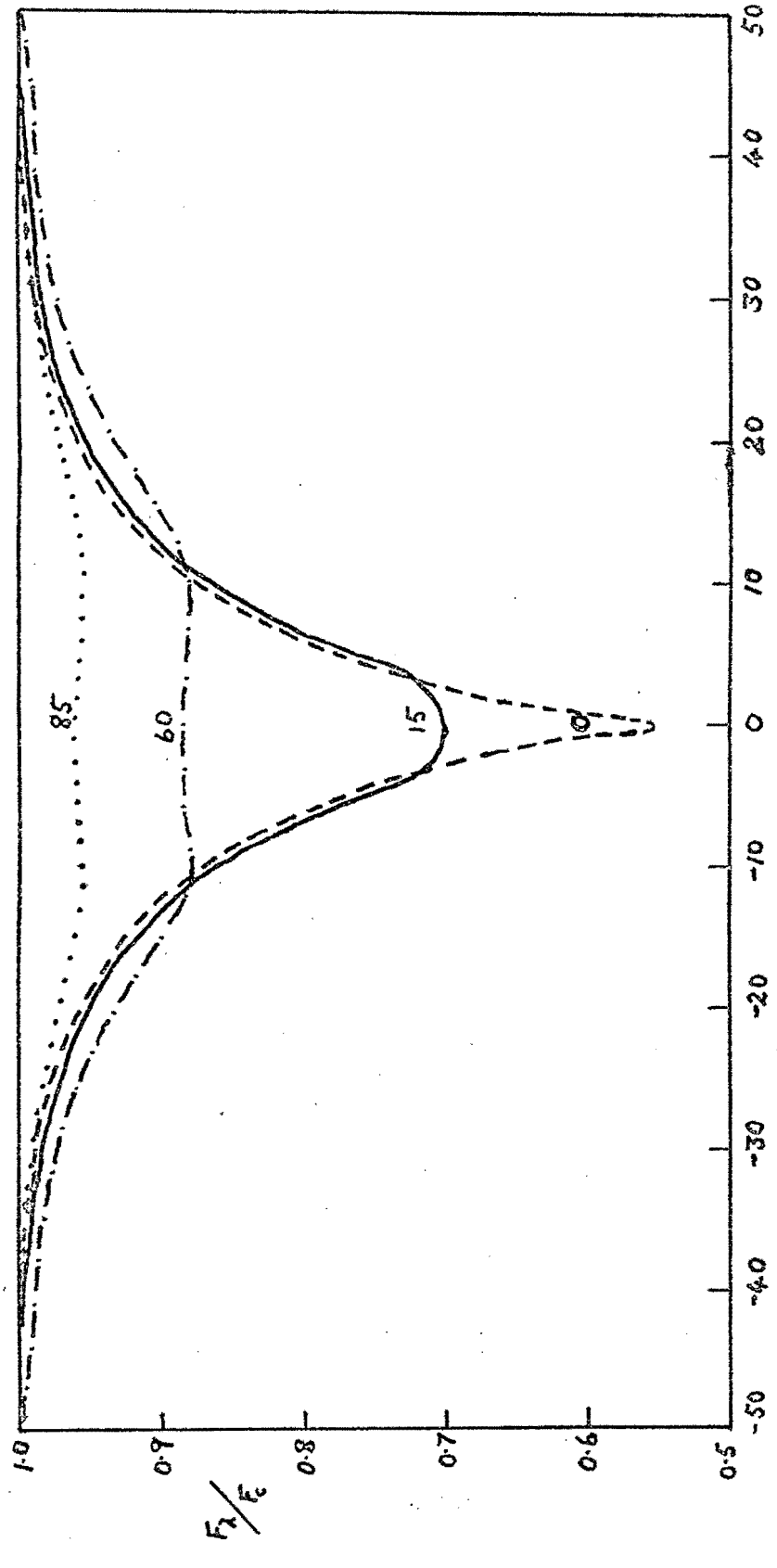

Figure 14. H_β absorption line profiles for model 3 with $R_d = 27\ R_s$

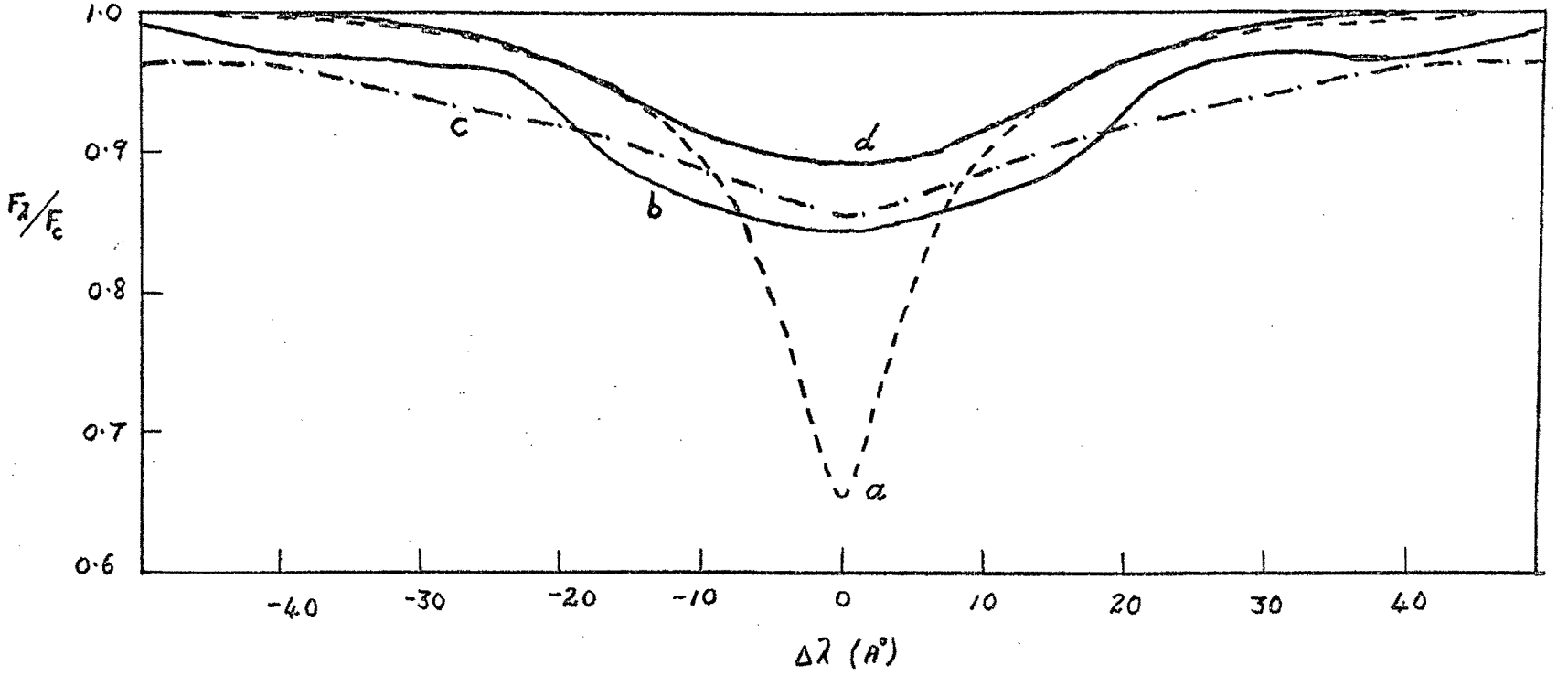

Figure 15. Observed hydrogen absorption line profiles

(a) mean H_γ - H_δ profile of LS 63° - 198

(b) H_γ in SW UMa (c) H_γ in CD - 42° 14462

(d) Mean H_γ - H_δ profile for LS 55° - 8

(see text for references)

(iii) The same mechanism is responsible for the shallowness of lines in model 2.

(iv) Equivalent widths decrease with increasing inclination. This is caused by limb darkening (presence of sec i in equations (3.1.1) and (3.1.2)).

(v) The total widths of the lines are relatively insensitive to the inclination of the disk. This is as a result of the increased broadening by the rotational Doppler (equation (3.1.3)) competing with a reduction in line depth by limb darkening at high inclinations.

Although differences between line shapes are not sufficient to rule out any model conclusively, the qualitative agreement with published profiles is at least encouraging. In particular, the curves with $i = 30^{\circ}$ in model 2 ($R_d = 14\ R_s$) and $i = o$ in model 2 ($R_d = 30\ R_s$) resemble the mean $H_\gamma - H_\delta$ profiles of LS 55° - 8 and LS 63° - 198 respectively (Greenstein et al. 1970). The two calculated profiles have central depths $A_c \sim 10.5\%$ and 36%, total widths $\omega_t \sim 70$ Å and 80 Å and widths at half maximum absorption $\omega_{\frac{1}{2}} \sim 28$ Å and 11 Å. This should be compared with the published curves which have $A_c \sim 11\%$, $\omega_t \sim 75$ Å, $\omega_{\frac{1}{2}} \sim 32$ Å (LS 55° - 8) and $A_c \sim 35\%$, $\omega_t \sim 86$ Å, $\omega_{\frac{1}{2}} \sim 12$ Å (LS 63° - 198). The $i = 30^{\circ}$ curve in model 2 ($R_d = 14\ R_s$) also corresponds qualitatively with the H_δ and H_ε profiles of TT Ari shown in a paper by Cowley et al. (1975). These lines have $\omega_t \sim 50 - 70$ Å and $A_c \sim 9 - 11\%$. (Note that the authors found $30^{\circ} \lesssim i \lesssim 40^{\circ}$.)

Agreement with the H_γ profile of SW U Ma obtained by Wellmann (1952) ($\omega_t \sim 100$ Å, $\omega_{\frac{1}{2}} \sim 36$ Å and $A_c \sim 16\%$) is also

reasonable. With reference to this, see the $i = 45^{\circ}$ curve of model 1 ($R_d = 21\ R_s$) which has $\omega_t \sim 90$ Å, $\omega_{\frac{1}{2}} \sim 36$ Å and central depth ~ 14.5%. Cowley & MacDonnell (1972) reported values very similar to these theoretical results for the hydrogen spectrum of BD - $7^{\circ}3007$: $\omega_{\frac{1}{2}} \sim 35$ Å and maximum central absorption ~14% for H_β. (For convenience some of the observed profiles are reproduced in figure 15.)

With the exception of LS 63° - 198 all the objects mentioned above are either established or suspected CVs; the results lend support to the suggestion of Warner (1976) that broad, shallow lines observed in CV-systems originate in the disk.

For broadening mechanisms other than those taken into account:

(i) $\frac{N_o}{N_e} < 10^3$ throughout the atmospheres of all three model disks, so resonance broadening may be neglected.

(ii) The unimportance of quadratic Stark absorption is guaranteed by the fact that $N_e \lesssim 10^{17}$ always holds.

(iii) Radiation damping is obviously negligible, although it is sometimes more important than resonance broadening.

Checks reveal that the ratio $\frac{N_i}{N_e}$ can be as low as 0.85. This implies that the Stark absorption in the near wings has sometimes been overestimated by up to ~ 11%. In the electron-dominated far wings, errors cancel. The effect should not be too serious as hydrogen is appreciably ionized under these conditions.

Results for $\alpha > 1$

Solutions for models with $\dot{M} = 10^{17}$, 10^{18} g sec^{-1} and supersonic turbulent velocities were obtained at a few radial positions. The following results are of note:

(i) The central temperature T_o and density ρ_o are both lowered drastically in comparison to the subsonic model results. Two causes are apparent: (a) the increased viscosity leads to a faster radial flow of material; consequently there is less accumulation of mass in the disk, and (b) the turbulent pressure thickens the disk so that the concentration of material in it is lowered.

(ii) For $\dot{M} = 10^{18}$, $\alpha \gtrsim 18$ the region $r \gtrsim 4$ of the disk is optically thin. Even for $\alpha = 18$, the SS viscosity is smaller than η_t predicted by Ter Haar $\left(\frac{\eta(SS)}{\eta(TH)} \sim 0.2\right)$ and Von Kármán $\left(\frac{\eta(SS)}{\eta(VK)} \sim 6 \times 10^{-2}\right)$ in the $r \gtrsim 4$ part of the disk.

(iii) The models $\dot{M} = 10^{17}$, $\alpha \gtrsim 8$ are optically thin for $r > 16$. If $\alpha \gtrsim 14$, the region $r \gtrsim 4$ has $\tau_o < 1$. The model $\alpha = 8$ has $\frac{\eta(SS)}{\eta(TH)} \sim 2.7 \times 10^{-3}$ and $\frac{\eta(SS)}{\eta(VK)} \sim 8 \times 10^{-3}$ $(16 \lesssim r \lesssim 20)$.

(iv) The extent of the convection regions in the disk is decreased compared with $\alpha \lesssim 1$ models because of the reduction in τ_o. For example, if $\alpha = 2$, $M = 10^{17}$ g sec^{-1} only the region $0.03 \lesssim y \lesssim 0.213$ at $r = 20$ is convective; this should be contrasted with $0 \lesssim y \lesssim 0.89$ for model 1.

(v) The importance of radiation pressure increases when compared to models with $\alpha \lesssim 1$, e.g. the model $\alpha = 14$, $\dot{M} = 10^{18}$

has $0.5 \lesssim \frac{P_r}{P_g}$ $(Z = o) \lesssim 0.9$ for $4 \lesssim r \lesssim 16$.

(vi) Turbulent conduction appears to play a similar role to that in $\alpha \lesssim 1$-disks: $0.46 \lesssim \frac{q^{(t)}}{q^{(r)}}$ $(Z = o) \lesssim 0.54$ ($\alpha = 8$, $\dot{M} = 10^{18}$, $10 \lesssim r \lesssim 15$) and $0.48 \lesssim \frac{q^{(t)}}{q^{(r)}}$ $(Z = o) \lesssim 0.59$ ($\alpha = 4$, $\dot{M} = 10^{17}$, $4 \lesssim r \lesssim 12$).

(vii) The vertical scale in the disk increases with increasing α, but the thin-disk assumption remains approximately valid even when the disk becomes optically thin. Thus $^{Z}o/R < 0.09$ ($\alpha = 6$, $\dot{M} = 10^{17}$, $r > 16$) and $^{Z}o/R < 0.33$ ($\alpha = 18$, $\dot{M} = 10^{18}$, $4 \lesssim r \lesssim 24$).

(viii) The corresponding ratios $\frac{|V_r|}{V_\theta}$ for the two models are ~ 0.02 and ~ 0.37.

Since the viscosity laws of Ter Haar and Von Kármán correspond to very large values of α, (ii) and (iii) imply that the results to be expected from models using (1.2.4) or (1.2.5) would probably disagree with observations of optically thick disks.

VII. Conclusions

The three models constructed are all self-consistent in the sense that the assumptions made are satisfied within large margins. We note, however, that the models break down in the immediate vicinity of the star (e.g. equation (2.1.13)). Treatment of the region of interaction between the disk and the star is important especially for predicting the continuum radiation produced there. Radiation from the disk appears to be insufficient to account for the observed X-ray flux (fig. 5). It seems likely, therefore, that it should be generated in either the boundary layer or the hot spot or perhaps in both. Once reliable models for these two exotic regions are available, and provided departures from the quasi-steady state are not too great, it should in principle be possible to determine the mass transfer rate through the disk from the continuum radiation distribution.

It appears that the viscosity laws of Von Kármán and Ter Haar can be rejected as these lead to optically thin disks. This conclusion is provisional, as the thin-disk approximation does not hold for corresponding extreme values of α.

Clearly (figures 3, 7 and 8) the geometrical shape of the disk is not conducive to reflection of light produced in the disk. Radiation from the star might however be reflected off the disk. Bearing in mind the crudeness of the models, it would seem that the observed oscillations most likely originate in the primary. (The existence of ionization zones in the disk also opens the interesting possibility of pulsations in the disk itself via the usual Cepheid mechanism.)

Since electron scattering is unimportant in all models, polarization of radiation would probably imply the existence of magnetic fields in the system.

The reasonable qualitative agreement of line profiles calculated here with some observed line shapes shows that the latter might indeed be formed in disks. If this is so, a number of possibilities exist.

(i) Since different parts of our profiles originate in distinct areas in the disk, observations might be used to gain an idea of the radial variation of disk parameters.

(ii) Once the situation as regards the viscosity in the disk has been cleared up, better calculations (e.g. convolution of Doppler and Stark profiles, more accurate Stark broadening tables, etc.) might be used in a spectroscopic search for CVs.

(iii) Profiles could be used to estimate the inclinations and sizes of disks.

Two methods for discriminating between Stark-broadened lines originating in the white dwarf and Doppler-broadened lines from the disk may be possible:

(i) At high inclinations a slight rise ($\lesssim$ ½%) is apparent in the line centres of our profiles. (This might be undetectable with present techniques.)

(ii) During eclipse of disks of high inclination the shape of lines originating in the disk would be altered drastically as approaching or receding parts of the disk are obscured.

The models discussed here could easily be developed further. Thus a more detailed treatment of convection and ionization, the use of different stellar parameters and the computation of the profiles of other absorption lines and of equivalent widths might reveal useful features. Parameters found here could also be used in a thorough investigation of shock wave propagation in the disk in order to test the suggestion of Starrfield et al. (1974a,b) and Warner (1974) concerning the outburst mechanism.

By making suitable changes to M_s , R_s and the opacity, a long overdue application to other systems containing disks or rings (e.g. solar disk, Be-rings, etc.) could be made. In this way a large number of new observational tests should become available.

Before all this is attempted, however, the question of stability against turbulence should be studied more carefully. Two methods can be suggested: (a) a numerical stability analysis of a laminar model and (b) in the absence of turbulence, it is possible that only disks with mass transfer rates below $\sim 10^{18}$ g sec^{-1} will show "chromospheric" emission lines. If emission lines are observed in all cases, chromospheric models could yield information about the nature of turbulence in the disk (Icke 1975). (Fortunately it seems possible to separate emission lines produced in the disk from those associated with the hot spot - see Smak (1975.)

Three observational facts do not agree very well with results presented here:

(i) The disk is thought to be geometrically thick (Smak 1971). If the disk is indeed as thin as our models predict, the white dwarf should be visible even at small inclinations - careful analysis of data might settle this question. On the other hand, thicker disks will be obtained if α is reduced or in laminar models.

(ii) The disk mass is thought to be larger than the values obtained here. As we have pointed out, observations might be in error on this point. The situation could be clarified by using the suggestion of Sparks & Starrfield (1975) (that the geometrical shape of nova shells is caused by an interaction between the ejected material and the disk) as a basis for an estimate of M_d . A more careful analysis along the lines of Warner's calculation might also be helpful.

(iii) The total widths of some of the observed absorption lines are far in excess of widths calculated here (e.g. Wegner (1972), Greenstein (1957)). This might be remedied by changing the stellar parameters used for our calculations. (In particular, raising the mass of the white dwarf would increase the Keplerian velocity in the disk; this would give rise to larger rotational Doppler broadening of the lines. On the other hand, the increase in the tangential stress would cause the disk to be hotter so that the inner regions (where rotational Doppler broadening is most important) could be too ionized to produce significant line absorption.) If there is still no agreement, it might indicate that (a) these lines are not associated with the disk or (b) that the models must be revised.

References

Allen, C.W., 1973. *Astrophysical Quantities*, Athlone Press, London.

Aller, L.H., 1963. *Astrophysics*, Ronald Press, New York.

Batchelor, G.K., 1955. Vistas in Astronomy 1, 290.
1958 in *Cosmical Gas Dynamics* (eds. J.M. Burgers & R.N. Thomas).

Bath, G.T., 1973. Nature Phys. Sci. 244, 84.

Bath, G.T., Evans, W.D., Papaloizou, J. & Pringle, J.E., 1974. M.N.R.A.S. 169, 447.

Bath, G.T., Evans, W.D. & Pringle, J.E. 1974a. M.N.R.A.S. 166, 113.

Bath, G.T. & Papaloizou, J.,1975. M.N.R.A.S. 172, 339.

Bode, G.,1965. *Kontinürlicke Absorption von Sternatmosphären*, Kiel.

Chandrasekhar, S., 1939. *An Introduction to the Study of Stellar Structure*, University of Chicago Press, Chicago.
1949. Ap. J. 110, 329.
1961. *Hydrodynamic and Hydromagnetic Stability*, Oxford University Press, London.

Chapman, S. & Cowling, T.G., 1960. *The Mathematical Theory of Non-Uniform Gases*, Cambridge University Press, London.

Cowley, A.P. & MacDonnell, D.J., 1972. Ap. J. Lett. 176, L27.

Cowley, A.P., Crampton, D., Hutchings, J.B. & Marlborough, J.M., 1975. Contr. Dominion Astrophys. Obs. No. 237.

Cox, A.N. & Stewart, J.N., 1970. Ap. J. Suppl. 19, 243.

Cox, J.P. & Giuli, R.T., 1968. *Principles of Stellar Structure (Vol. 1)*, Gordon & Breach, New York.

Dallaporta, N. & Lucchin, F., 1972. Astron. & Astrophys. 19, 123.
1973. Astron. & Astrophys. 26, 325.

De Gregoria, A.J., 1974. Ap. J. 189, 555.

Doughty, N.H. & Fraser, P.A., 1966. M.N.R.A.S. 132, 267.

Eardly, D.M. & Lightman, A.P., 1975. Ap. J. 200, 187.

Eardly, D.M. & Lightman, A.P. & Shapiro, S.L., 1975. Ap. J. Lett. 199, L153.

Edmonds, F.M., Schlüter, H. & Wells, D.C., 1967. Mem. R.A.S. 71, 271.

Faulkner, J. 1971. Ap. J. Lett. 170, L99.
1974 in *Late Stages of Stellar Evolution* (ed. R.J. Taylor), Reidel.

Flannery, B.P., 1974. Ph.D.-thesis, University of California.

Glasby, J.S., 1969. *The Dwarf Novae*, Constable, London.

Gorbatsky, V.G., 1965. Soviet Astronomy - A.J. 8, 680.
1969 in *Non-Periodic Phenomena in Variable Stars* (ed. L. Detre), Academic Press, Budapest.

Greenstein, J.L., 1957. Ap. J. 126, 23.

Greenstein, J.L., Sargent, A.I. & Haug, U. 1970. Astron. & Astrophys. 7, 1.

Griem, H., Kolb, A.C. & Shen, K.Y., 1959. Phys. Rev. 116, 4.

Harrison, E.R., 1973. Ann. Rev. Astron. Astrophys. 11, 155.

Harwood, J. , 1973. M.Sc.-thesis, University of Cape Town.

Heise, J., Brinkman, A.C., Schrijver, J., Mewe, R., Groneschild, E., & Den Boggende, A., 1975. IAU Symposium No. 73.

Henry, P., Cruddance, R., Lampton, M., Paresce, F. & Bowyer, S. 1975, Ap. J. Lett. 197, L117.

Hinze, J.O., 1959. *Turbulence*, McGraw-Hill, New York.

Holm, A.V. & Gallagher, J.S., 1974. Ap. J. 192, 425.

Icke, V., 1975. IAU. Symposium, No. 73.

Kraft, R.P., 1963. Adv. Astron. & Astrophys. 2, 43.

Krzeminsky, W. & Smak, J., 1971. Acta Astr. 21, 133.

Landau, L.D. & Lifschitz, E.M., 1959. *Fluid Mechanics*, Pergamon Press, London.

Lighthill, M.J., 1953. Proc. Cambridge Phil. Soc. 49, 531. 1955 in *Gas Dynamics of Cosmic Clouds*, North Holland Publishing Co., Amsterdam.

Lightman, A.P., 1974a. Ap. J. 194, 419.

1974b. Ap. J. 194, 429.

Lortet, M.C., 1969 in *Non-Periodic Phenomena in Variable Stars* (ed. L. Detre), Academic Press, Budapest.

Lynden-Bell, D., 1969. Nature 223, 690.

Lynden-Bell, D. & Pringle, J.E., 1974. M.N.R.A.S. 168, 603.

Mihalas, D., 1970. *Stellar Atmospheres*, W.H. Freeman & Co., San Fransisco.

Mitchner, M. & Kruger, C.H., 1973. *Partially Ionized Gases*, John Wiley & Sons, New York.

Mumford, G.S., 1967. P.A.S.P. 70, 283.

Münch, G., 1960 in *Stellar Atmospheres* (ed. J.L. Greenstein), University of Chicago Press, Chicago.

Nather, R.E. & Robinson, E.L., 1974. Ap. J. 190, 637.

Osaki, Y., 1974. Publ. Astron. Soc. Japan 26, 429.

Page, D.N. & Thorne, K.S., Ap. J. 191, 499.

Payne-Gaposchkin, C., 1964. *The Galactic Novae*, Dover, New York.

Prendergast, K.H. & Burbidge, G.R., 1968. Ap. J. Lett. 151, L83.

Pringle, J.E., 1973. N.Y. Acad. Sci. Ann. 224, 280.

1974 Ph.D.-thesis, University of Cambridge.

1975 M.N.R.A.S. 170, 633.

Pringle, J.E. & Rees, M.J., 1972. Astron. & Astrophys. 21, 1.

Rappaport, S., Cash, W., Doxsey, R., McClintock,J. & Moore, G., 1974. Ap. J. Lett. 187, L5.

Rees, M.J., 1975. M.N.R.A.S. 171, 457.

Robinson, E.L. , 1973. Ap. J. 186, 347.

Schaaf, S.A., 1963 in *Handbuch der Physik* (ed. S. Flügge), Springer-Verlag, Berlin.

Schlichting, H., 1968. *Boundary Layer Theory*, McGraw-Hill, New York.

Shakura, N.I., 1973. Soviet Astr.-AJ 16, 756.

Shakura, N.I. & Sunyaev, R.A., 1973. Astron. & Astrophys. 24, 357.

Smak, J., 1969. Acta Astron. 19, 155.
1971. Acta Astron. 21, 15.
1972. Acta Astron. 22, 1.
1975. IAU Symposium, No. 73.

Sparks, W.M. & Starrfield, S. 1973. M.N.R.A.S. 164, 1P, 1975 Preprint

Starrfield, S., Sparks, W.M., Truran, J.W., Kutter, G.S., 1972. Ap. J. 176, 169.

Starrfield, S., Sparks, W.M. & Truran, J.W., 1974a. Ap. J. Suppl. 261, 247.
1974b. Ap. J. 192, 643.

Stewart, J.M., 1975. Astron. & Astrophys. 42, 95.

Swihart, T., 1956. Ap. J. 123, 143.

Szkody, P.,1974. Ap. J. Lett. 192, L75.

Ter Haar, D., 1950. Ap. J. 111, 179.

Thorne, K.S., 1974. Ap. J. 191, 507.

Von Kármán, T., 1956. *Collected Works*, Butterworths, London.

Von Weizsäcker, C.F., 1951. Ap. J. 114, 165.

Walker, M.F. & Chincarini, G., 1968. Ap. J. 154, 157.

Warner, B., 1973. Sky Telesc. 46, 298.

1973a. M.N.R.A.S. 162, 189.

1974. M.N.R.A.S. 168, 235.

1976. Preprint (To be published in Observatory)

Warner, B. & Robinson, E.L., 1972. Nature Phys. Sci. 239, 2.

Wegner, G., 1972. Astrophys. Lett. 12, 219.

Wellmann, P., 1952. Zs. f. Ap. 31, 123.